NOTE TO USERS

uOttawa

L'Université canadienne
Canada's university

FACULTÉ DES ÉTUDES SUPÉRIEURES ET POSTOCTORALES

uOttawa

L'Université canadienne
Canada's university

FACULTY OF GRADUATE AND POSDOCTORAL STUDIES

Matthew Tang
AUTEUR DE LA THÈSE / AUTHOR OF THESIS

M.Sc. (Biochemistry)
GRADE / DEGREE

Department of Biochemistry, Microbiology and Immunology
FACULTÉ, ÉCOLE, DÉPARTEMENT / FACULTY, SCHOOL, DEPARTMENT

Gene Reprogramming by K48R Mutant Ubiquitin in a Mouse Model of SCA1

TITRE DE LA THÈSE / TITLE OF THESIS

Doug Gray
DIRECTEUR (DIRECTRICE) DE LA THÈSE / THESIS SUPERVISOR

CO-DIRECTEUR (CO-DIRECTRICE) DE LA THÈSE / THESIS CO-SUPERVISOR

EXAMINATEURS (EXAMINATRICES) DE LA THÈSE / THESIS EXAMINERS

Alex MacKenzie

Valerie Wallace

Gary W. Slater
LE DOYEN DE LA FACULTÉ DES ÉTUDES SUPÉRIEURES ET POSTDOCTORALES /
DEAN OF THE FACULTY OF GRADUATE AND POSTDOCORAL STUDIES

Gene Reprogramming by K48R Mutant Ubiquitin in a Mouse Model of SCA1

Matthew Y. Tang

Thesis submitted to
the Faculty of Graduate and Postdoctoral Studies
in partial fulfillment of the requirements for the degree of
Master's in Biochemistry

Department of Biochemistry, Microbiology and Immunology
Faculty of medicine
University of Ottawa

Your file Votre référence
ISBN: 0-494-11426-6
Our file Notre référence
ISBN: 0-494-11426-6

Abstract

Spinocerebellar ataxia type 1 (SCA1) is an incurable neurodegenerative disease resulting from the loss of Purkinje neurons within the cerebellum. The causative agent of the disease is the expansion of a trinucleotide repeat in its gene product ataxin-1. The ubiquitin proteasome pathway (UPP) has been implicated in SCA1 but the role of proteolysis in the disease is still poorly understood. To further investigate this issue *in vivo,* genetic crosses were performed between a well established mouse model of SCA1 and novel strains expressing elevated levels of wild type or mutant isoforms of ubiquitin. The K48R mutant isoform of ubiquitin (a dominant negative inhibitor of proteolysis) was found to significantly delay the deterioration of Purkinje neurons as evidenced by behavioral, morphological, and molecular indicators. This delay was accompanied by the restoration of genes involved in calcium and glutamate signalling and by the stabilization of postsynaptic density proteins whose abundance/activity would otherwise decline in the course of the SCA1 disease. These results are consistent with transcriptional dysregulation as a key mechanism in neurodegeneration and suggest that the UPP is a useful target for the development of novel therapies.

Acknowledgments

I am grateful to my supervisor Dr. Douglas A. Gray for his encouragement, advice, patience, guidance, and the opportunity for this Master's research project. I would like to thank him for sharing his unique ideas and passion for exquisite photography.

I would like to extend my thanks to Drs. John Woulfe, Bruce McKay and Rashmi Kothary for their role as thesis committee advisors providing me with constructive criticism with regards to experiments. Special thanks to Jamie and Ivan for their technical assistance with regards to the LightCycler®.

I would like to thank the members of the Gray laboratory (especially Tania Lefebvre, Jan Brun, James Villeneuve, Melissa Beyers, and Mei Zhang) and all members of the ORCC (especially Dr. Jim Dimitroulakos, Chris Kamel, Alenko, Brodie and Nima,) for their friendship, humour, countless soccer games and festivities during my stay in Ottawa.

I am indebted to Maria Tsirigotis for her endearing friendship, kindness and strong emotional support throughout the good and bad times we shared including 'Greek mafia coup de grace' attempts during our tenure as lab-rats in the Gray lab. I would also like to thank her for sharing her wisdom, philosophy, tireless commitment and enthusiasm for science, and for her editorial help during the process of writing the thesis.

I am sincerely thankful to Dr. K.T. Kan, a long time friend, mentor, and source of my inspiration for neuroscience.

With all my heart, I am forever grateful to my family especially Sephora, Mom, Dad, and the grandparents for their unwavering support.

One ought, every day at least, to hear a little song, read a good poem, see fine pictures, and, if it were possible, to speak a few reasonable words.

Johann Wolfgang von Goethe

Table of contents

CHAPTER 3: RESULTS

CHAPTER 4: DISCUSSION

List of Figures

List of tables

Abbreviations

AD	Alzheimer's disease
AMPA	Alpha-amino-3-hydroxy-5-methylisoxazole-4-propionic acid
AKT	Protein Kinase B
ALS	Amyotrophic lateral sclerosis
ATP	Adenosine triphosphate
Atx-1	Ataxin-1
BSA	foetal bovine serum
CamK-II	Calcium/calmodulin-dependent kinase II
cAMP	Cyclic adenosine monophosphate
CARP	Carbonic anhydrase-related protein
CBP	CREB binding protein
cDNA	Complementary dioxy-ribonucleotide
CMV	Cytomegalovirus
CREB	Cyclic AMP response element binding protein
C_T	Threshold cycle number
C-terminal	Carboxy-terminal
DAG	Diacylglycerol
DAPI	4',6-diamidino-2-phenylindole
DNA	Dioxyribonucleic acid
DUB	De-ubiquitinating enzymes
EDTA	Ethyl diamine-tetra-acetic acid
EEAT4	Glutamate excitatory amino acid transporter type 4
GFAP	Glial Fibrillary Acidic Protein
ER	Endoplasmic reticulum
GABA-A	gamma-aminobutyric acid receptor
Gly	Glycine
HAT	Histone acetyltransferase
HD	Huntington's disease
HDAC	Histone deacetylase
HMW	High molecular weight
HSP	Heat shock protein
IP3	Inositol 1,4,5-triphosphate
IP3R1	Inositol 1,4,5-trisphosphate receptor 1
ITPKC	inositol 1,4,5-trisphosphate 3-kinase C
Kb	kilobase
LPS	Lipopolysaccharide
LTD	Long term depression
LTP	Long term potentiation
Lys	Lysine
mGluR	Metabotropic glutamate receptor
mRNA	Messenger RNA
NaCl	Sodium chloride
NAF	Sodium Fluoride
NaPPi	Sodium pyrophosphate
NFkB	Nuclear factor kB

NP-40	Nonidet P-40
N-terminal	Amino-terminal
PBS	Phosphate buffered saline
PCR	Polymerase chain reaction
PGHP	Post peptidyl-glutamyl hydrolytic
PIB5P	Phosphatidylinositol (4,5) bisphosphate 5-phosphatase
PKC	Protein kinase C
PKCγ	Protein kinase C gamma isoform
PLC	Phospholipase C
PMSF	Phenylmethylsulphonyl fluoride
Poly Q	Polyglutamine
PP2A	Protein phosphates 2A
PSD	Postsynaptic density
RGS	Arginine-Glycine-Serine
ROS	Reactive oxygen species
SCA1	Spinocerebellar ataxia 1
SDS	Sodium dodecyl sulfate
SDS-PAGE	Sodium dodecyl sulfate polyacrylamide gel electrophoresis
SERCA	Sarcoendoplasmic reticulum Ca^{2+}-ATPase type 2
SV40	Simian virus 40
TBST	Tris buffered saline with Tween-20
TRIS	Tris (hydrozymethyl) aminomethane
Ub	Ubiquitin
UbC	Ubiquitin C
UBP	Ubiquitin specific protease
UCH	Ubiquitin carboxy-terminal hydrolase
UPP	Ubiquitin proteasome pathway
VGCC	Voltage gated calcium channels
Wt	Wild-type

Chapter 1

Introduction

1.1 The ubiquitin-proteasome pathway

The ubiquitin-proteasome pathway (UPP) is responsible for the rapid and irreversible elimination of proteins. It is a tightly regulated process with a high degree of specificity. A simplified schematic diagram of the UPP is show in Figure 1 (Gray et al., 2003). Ubiquitin (depicted in Figure 2), a highly conserved 76 amino acid protein, serves as a covalent tag to direct molecule protein substrates (either normal or misfolded/damaged proteins) for degradation through a series of consecutive steps involving ubiquitin metabolizing enzymes (E1, E2, and E3). The initial step involves the activation of the C-terminal glycine residue of ubiquitin by an ubiquitin activating enzyme E1 in a step dependent on ATP. This reaction converts ubiquitin into a high-energy thioester intermediate (E1-S~ubiquitin). The activated intermediate is then transferred to an ubiquitin-carrier protein E2 which, with the assistance of an E3 ligase, attaches the Gly76 of the ubiquitin moiety via an isopeptide bond to an internal lysine of a target substrate. The efficient targeting of the protein structure to the 26S proteasome is dependent on the formation of a threshold length polyubiquitin chain assembled through the Gly76 of one ubiquitin moiety to Lys48 of the preceding ubiquitin molecule. Thus, successive rounds of ubiquitylation are required for efficient targeting and degradation of the protein to the 26S proteasome where it is degraded in the inner compartment of the protease (Glickman and Ciechanover, 2002).

Figure 1. Schematic representation the UPP

The covalent attachment of ubiquitin to a protein substrate (either a normal protein destined for degradation or a damaged or abnormally folded protein) proceeds via a three-step cascade. In an initial reaction, the C-terminal G76 of ubiquitin is activated by an ubiquitin activating enzyme. This reaction is followed by substrate recognition and subsequent addition of an ubiquitin moiety to the substrate, a step mediated through interactions between E2 conjugases and E3 ligases, respectively. The mono-ubiquitination of the substrate is followed by successive addition of other ubiquitin moieties through the formation of an isopeptide bond between K48-G76 to form a polyubiquitin chain. The recognition of a threshold length polyubiquitin chain by the proteasome ensures its unfolding and degradation by the proteolytic activities lining the inner rings of the protease. Deubiquitination enzymes (DUBs) recycle ubiquitin by releasing ubiquitin from the polyubiquitin chain assembled on the substrate yielding free ubiquitin monomers.

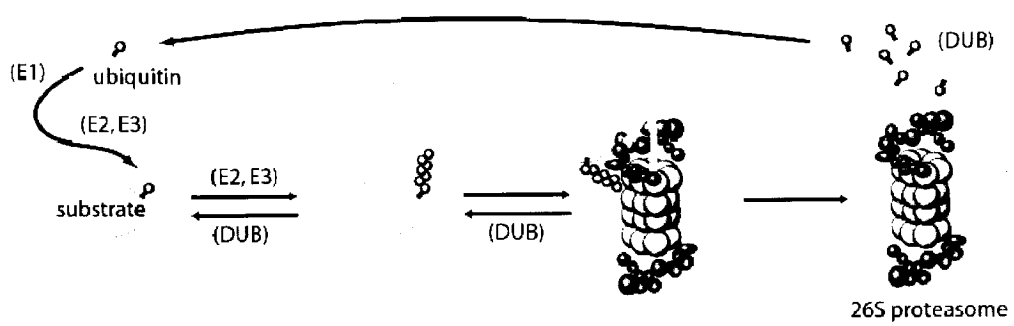

Gray et al, SAGEKE, 2003

Figure 2. Three-dimensional structure of ubiquitin

Schematic representation of the 76 amino acid ubiquitin monomer revealing a compact N-terminus composed of α-helices and β-sheets. The structure also reveals a more flexible, less structured protruding C-terminus consisting of only 6 amino acids.

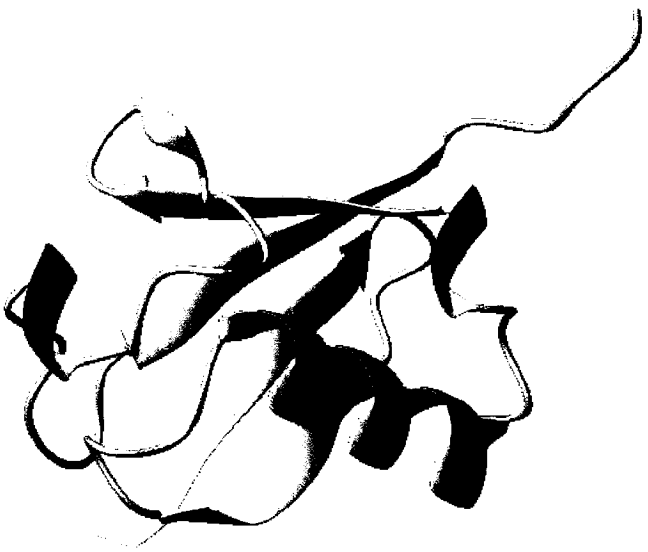

http://darwin.chem.nottingham.ac.uk/group/protein.html

1.2 The 26S proteasome

The 26S proteasome (depicted in Figure 3) is a ubiquitously expressed, ATP-dependent cytoplasmic and nuclear multi-subunit enzyme protease charged with the elimination of cellular protein substrates. It has a molecular mass of approximately 2.5 MDa and can functionally divided in a core (20S) particle and a regulatory particle (19S) that caps either end of the 20S particle. The cap can be further divided in a base and a lid component (reviewed in (Pickart and Cohen, 2004)).

1.2.1 The 20S core particle

The 20S proteasome in eukaryotes is composed of two distinct subunits: the ß-type subunits which contain the catalytic activities and the α-type which are required for structural reasons (reviewed in (Hilt and Wolf, 1995)). Three distinct proteolytic activities have been associated with the 20S proteasome; the trypsin-like, the chymotrypsin-like, and the post-glutamyl peptidyl hydrolytic (PGPH) activities which cleave after basic, large hydrophobic and acidic residues respectively (Orlowski et al., 1993). The 20S proteasome has been shown to have proteolytic cleavage towards denatured or oxidized proteins (without requirement for ATP, (Shringarpure et al., 2003)).

1.2.2 The 19S particle

The 19S complex is composed of a lid and a base that caps the ends of the 20S proteasome; the base contains six ATPases and three non-ATPases (Rpn1,2 and 10) while the lid is composed of eight non-ATPase subunits (Rpn3,5,6,7,8,9,11 and 12) that serve in the recognition of ubiquitylated substrates (Glickman et al., 1998) and reviewed in (Hilt and Wolf, 1995)). The putative role of the base is one of a molecular chaperone

Figure 3. Organization of the eukaryotic 26S proteasome

A) Electron micrograph of the eukaryotic proteasome isolated from rat liver. The structure consists of two 19S regulatory particles that cap the 20S catalytic core. B) Schematic representation of A) showing the lid and base components that constitute the 19S regulatory particle.

A

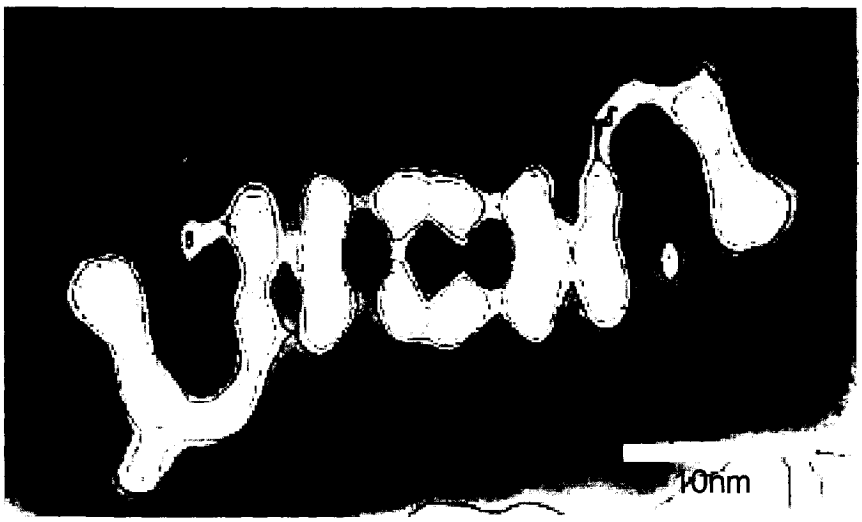

Yoshimura et al, 1993

B

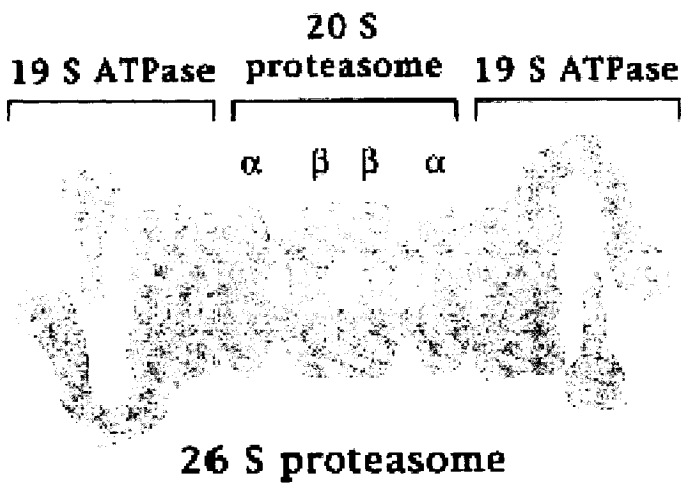

Kessel et al, 1995

involved in the unfolding and translocation of protein substrates into the catalytic chamber (Braun et al., 1999).

1.3 Roles of ubiquitin in non-proteolytic cellular processes

Polyubiquitin chains assembled through linkages other than G76-K48 have roles in processes that do not involve protein degradation. The formation of a linear K63 linked polyubiquitin chain has been recently implicated in the signalling of NF-κB transcription factor resulting in the activation of downstream genes (Deng et al., 2000), in endocytosis of membrane bound receptors destined for degradation in the lysosome, in DNA repair and in ribosome assembly (Glickman and Ciechanover, 2002). The disruption of K63 linked polyubiquitin chains in yeast has been shown to sensitize cells to radiation-induced damage and in defects in the error prone DNA repair pathway ((Arnason and Ellison, 1994) and (Spence et al., 1995)). The mono-ubiquitin signal (as opposed to polyubiquitin) plays a well documented role in transcriptional control whereby the attachment of a single ubiquitin to histone proteins modulates gene expression (Sun and Allis, 2002; Kao et al., 2004). Mono-ubiquitylation can serve in vesicular sorting in the endocytic pathway (Katzmann et al., 2001), as a sub-cellular localization motif (Plafker et al., 2004), in the internalization of membrane bound receptors (Haglund et al., 2002; Sun and Allis, 2002) and in viral budding (Patnaik et al., 2000).

1.4 Ubiquitin genes and the generation of monomeric ubiquitin

Ubiquitin is never expressed as a monomer but as a linear fusion of tandem repeats of ubiquitin or linear fusion between ubiquitin and ribosomal subunits. The UBA genes (UBA52 and UBA80) encodes the latter type of fusions whereas the UBB and UBC

genes are coding sequence in a spacerless head to tail arrangement (Redman and Rechsteiner, 1988; Baker and Board, 1991). The ubiquitin-ribosomal fusion proteins are ubiquitously expressed in all cells and provide the majority of ubiquitin in unstressed conditions. During conditions of stress, such as starvation or elevation of temperature, the UBB and UBC genes (which in most humans are comprised of 3 and 9 tandem repeats of ubiquitin respectively) are induced and elevate cellular ubiquitin pools thereby facilitating a rapid UPP response to deal with misfolded or damaged proteins . Both types of fusions are subject to co-translational processing to yield monomeric ubiquitin that can be attached to cellular proteins. Ubiquitin carboxy-terminal hydrolases (UCHs) and Ubiquitin specific proteases (UBPs), collectively refered to as deubiquitylating enzymes (DUBs) serve in the processing of ubiquitin fusion proteins (either ribosomal or polyubiquitin fusions), in the editing of poly-ubiquitin chains assembled on protein substrates (thereby affecting their steady state levels by removing ubiquitin and rescuing them from degradation), and in the recycling of ubiquitin from small adducts to replenish ubiquitin pools (Wing, 2003). Most DUBs are free floating enzymes although some have been associated with the 19S core particle of the proteasome where they serve in the disassembly and recycling of the polyubiquitin signal.

1.5 Ubiquitin and its role in transcriptional control

The role of ubiquitin in gene expression has been limited to the mono-ubiquitylation of histones and to the degradation of many transcriptional activators and components of the basal transcription machinery that are subject to ubiquitin mediated degradation by the 26S proteasome. It has been recently demonstrated that ubiquitin and ubiquitin components may play proteolytic and non-proteolytic roles in the regulation of gene

transcription (Muratani and Tansey, 2003). It has been shown that components of the basal transcription machinery exhibit E3 ubiquitin ligase activity or are associated with E3 ubiquitin ligases at the promoter of genes (Brower et al., 2002). In addition, deubiquitylating enzymes have been found at the same sites. These associations have been shown to result in the rearrangement of chromatin structure enabling the elongation of transcription by RNA polymerases. In addition to the presence of enzymes with ubiquitin activity, proteasomes have also been detected at the promoter of genes (mainly the 19S lid) suggesting a role of remodelling of chromatin by the ATPases found within this particle. All these observations have recently been summarized in a review from William Tansey (Muratani and Tansey, 2003) whose model stipulates that E3 ubiquitin ligases are recruited to the promoter of genes to modulate the activity of transcriptional activators (including RNA polyII). This interaction recruits proteasomes to the active sites and serve in the destruction of the gene activators to promote the elongation of transcription by RNA polII. The chaperone activity provided by the 19S subunits would serve to modify chromatin during transcription until its dissociation from the polymerase.

1.6 The role of ubiquitin in the maintenance of neuronal synapses

It is well documented that modifications occurring at synapses following synaptic activation are highly coordinated and dynamic (Perez-Otano and Ehlers, 2005). These molecular changes occurring at the synapse affect local gene expression, protein synthesis and destruction, processes required for neuronal plasticity. This mechanism has been shown to involve post synaptic density proteins, a family of proteins residing in the synaptic terminal. It has been shown that the composition of these PSD proteins is altered in response to activation and that the remodelling of the synapse is mediated by

the UPP (Ehlers, 2003). The ubiquitin dependent removal of key molecular regulators following synaptic activation facilitates dynamic changes in PSD structure and alters the morphology of the synapse suggesting an important role for the UPP in the rearrangement and maintenance of synapses to maintain plasticity in the mammalian brain.

1.7 The pathogenesis of SCA1, a protein folding disease

Spinocerebellar ataxia-1 (SCA1) is an autosomal dominant neurodegenerative disease that belongs to a large family of diseases collectively referred to as polyglutamine disorders. The clinical features of SCA1 include the loss of limb and gait coordination, imperfect articulation of speech that is accompanied by difficulties in breathing and swallowing (Orr, 2000). The causative agent is the expansion of a polyglutamine repeat within the gene product, ataxin-1 whose function remains unknown. The expression of a polyglutamine expanded ataxin-1 in animal models has been shown to recapitulate the features of the human disease via a mechanism of toxic gain of function. The length of the polyglutamine tract has been shown to be important in predicting the onset and severity of the disease with longer tracts having the most deleterious effects. Although the pathologically expanded protein is ubiquitously expressed in humans, pathological features are solely manifest in Purkinje cell neurons residing in the cerebellum and to a lesser extend in neurons of the brainstem. Purkinje specific expression of an expanded polyglutamine tract (tract of 82Qs) but not the non-expanded counterpart of 30Qs in mice has been shown to result in anomalies consistent with altered vesicle trafficking (including the presence of cytoplasmic vacuoles) and the presence of nuclear proteinaceous inclusions that are immunoreactive for ubiquitin and components of the

UPP (Orr, 2000). These pathological features can be alleviated by silencing the expression of transgene-derived ataxin-1 by RNAi (Xia et al., 2004).

It is become increasing clear that the presence of an expanded polyglutamine tract alters the conformation of gene product. This expansion has been shown to interfere with the clearance of the malfolded protein by the UPP and has been suggested to be the basis of its accumulation within the cells (Bence et al., 2001). This is consistent with the findings that exogenous expression of chaperone proteins in cultured cells expressing expanded polyQ proteins or in animal models of disease alleviates the phenotype and reduces inclusion formation by either chaperone-mediated refolding or targeting for degradation. If all else fails, the cell may sequester the toxic protein in an inclusion. Recent studies have suggested that the formation of inclusion bodies may be a protective cellular response to preclude association of the protein with cellular components and that coating ability of ubiquitin may play protective role in orchestrating inclusion formation (Arrasate et al., 2004). This protective role of inclusions is supported by findings that the presence of ubiquitylated aggregates does not correlate well with disease severity. For example, crossing a mouse model in which the E6-AP ubiquitin ligase has been knocked-out to the mouse model of SCA1 results in fewer inclusions but more pronounced pathology (Cummings et al., 1999). These observations have suggested that the elimination of ubiquitin components serves to aggravate the disease.

Combined with its increased stability (due to a failure to be cleared) it has been suggested that the altered conformation adapted by the aberrantly folded protein increases its propensity to aggregate and inadvertently interact with neuronal proteins to form

aggregates. Aggregates, being distinct from inclusions, are viewed as toxic entities due to their ability to interact with cellular components. It has been suggested that specific protein-protein interactions between ataxin-1 and cellular proteins may be the basis for its increased stability and its ability to exert its toxic effects. For example, serine phosphorylation of ataxin-1 by AKT has been found to increase its ability to bind the 14-3-3 protein (a protein that regulates the phosphorylation of specific target proteins) (Chen et al., 2003). This interaction has been shown to enhance the stability of the expanded protein and contribute to its toxicity. Likewise, the expanded polyglutamine tract has been shown to interact with and adversely affect the function of transcriptional factors and co-factors resulting in an altered gene expression. Consistent with this is the finding that the nuclear localization of ataxin-1 is necessary to result in pathology and that ataxin-1 has been shown to bind RNA (Irwin et al., 2005).

There is evidence to suggest that regions surrounding the polyglutamine expansion play important role in the pathogenesis of SCA1. This is supported by findings in which the high levels of exogenous expression of non pathological ataxin-1 with 30 polyglutamine repeats can result in neuronal degeneration (Fernandez-funez et al., 2000). Similarly, the expression of the AHX domain of ataxin-1, rather than the expression of the expanded polyglutamine tract, results in a gain-of-function of the protein by facilitating its interaction with transcriptions factors.

1.8 The aims of the research

The role of ubiquitin mediated proteolysis in neurodegeneration has remained elusive and is based primarily on findings performed in cultured mammalian cells expressing toxic

proteins. In order to obtain a better understanding of *in vivo* role of the UPP in modulating the course of disease, transgenic mice expressing either wild-type or mutant forms of ubiquitin were generated and bred to the well characterized mouse model of SCA1 (Tsirigotis et al., 2005, in press). The analysis of compound transgenic mice revealed that the introduction of a chain terminating version of ubiquitin (K48R) conferred protective effects and alleviated the anomalies readily observed in SCA1 mice. Taken together, the data suggest that perturbations in ubiquitin may prove beneficial in delaying neurodegeneration through mechanisms involving the restoration of gene transcription and/or by stabilizing key molecular proteins whose loss figures in disease.

Chapter 2

Materials and Methods

2.1 Generation of Transgenic Mice

Wt Ub-EGFP, K48R Ub-EGFP, and K63R Ub-EGFP ubiquitin transgenic lines were generated in the transgenic core facility of Dr. Barbara Vanderhyden (Ottawa Health Research Institute) by Manon Dube and have been previously described ((Tsirigotis et al., 2001b), (Zhang et al., 2003)). The B05 transgenic line carrying an expanded polyglutamine repeat of 82 codons within the gene product ataxin-1 and the A02 line with a repeat of 30 codons within the same gene were generated in the laboratory of Dr. Harry Orr (Burright et al., 1995), from whom the lines were obtained. Compound transgenic mice were obtained by crossing A02 and B05 mice with either wt Ub-EGFP, K48R Ub-EGFP or K63R Ub-EGFP ubiquitin transgenics.

2.2 Handling and processing of animal tissues

Animals were anaesthetized using CO_2 and sacrificed by cervical dislocation. Whole brains or cerebella of nontransgenic and transgenic animals were carefully excised and prepared accordingly for proteome, transcriptome or immunohistochemical analysis. Either tail clips or ear clips were used for genotyping purposes.

2.3 DNA extraction

Tail or ear clips derived from nontransgenic, wt Ub-EGFP, K48R Ub-EGFP, or K63R Ub-EGFP transgenic animals were incubated overnight at 50°C in 500µl of DNA extraction buffer (75mM NaCl, 25mM EDTA, 10mM Tris, 1% SDS) and 12.5µl of proteinase K (10mg/µl). Subsequently, the samples were vortexed and an equal volume (500µl) of 24:24:1 phenol: chloroform: isoamylalcohol (Sigma, St. Louis, Missouri, USA) was added and samples were mixed for 15 minutes at room temperature. Samples were

centrifuged at 14 000 RPM for 15 minutes at 4°C and the supernatant was removed and placed into a new tube containing 500µl of isopropanol. The mixture was then centrifuged at 14 000 RPM for 15 minutes at 4°C to pellet the DNA. The supernatant was discarded and the DNA pellet was washed with 500µl of 70% ethanol. Samples were then centrifuged at 14 000 RPM for 15 minutes at 4°C to pellet the DNA prior to allowing the DNA pellet to air dry. The pellet was resuspended in TE buffer (10mM Tris, 1mM EDTA, pH 8.0) and was quantified using a spectrophotometer (Eppendorf BioPhotometer).

2.4 Genotyping of various ubiquitin transgenics

Genotyping of the various transgenic mouse lines was achieved by Real-Time PCR using using the LightCycler® 1.5 instrument and SYBR Green I as the detection format (Roche Molecular Biochemicals, Mannheim, Germany). A forward primer sequence spanning the region of the transgene corresponding to K48, mutant K48R, K63, or mutant K63R were used in conjunction with a reverse primer that recognized a sequence in EGFP. Each primer set was tested with DNA derived from each ubiquitin transgenic resulting in a total of 4 distinct PCR reactions per DNA template. The successful amplification of DNA (as visualized by melting curve analysis or running the PCR product on a SDS-PAGE gel) with a given primer set was used as the determinant of the genotype of the animal. The primer sets used for the genotyping were as follows: forward primer for K48 5′-GCAGGCAAGCAGCTGGAA-3′; forward primer for K48R 5′AGGCCGGCAGCTGGAA-3′; forward primer K63 5′-ATCCAGAAAGAGTCGACCCTG-3′; forward primer for K63R 5′-AACATCCAGCGGGAGTCG-3′ and the reverse primer for EGFP 5′-CTTGCCGGTGGTGCAGAT-3′. The following LightCyler® cycling conditions were

used: (i) denaturation program (97 °C for 30 s); (ii) amplification and quantitation program repeated 35 times (97 °C for 2 s; 65 °C for 8 s; 72 °C for 9 s with a single fluorescent measurement); (iii) melting curve program (65–99 °C continuous fluorescent measurement); and (iv) cooling step to 40 °C. PCR conditions were as follows: 50ng of DNA combined with 4pmol of each primer (forward and reverse) and 2.0µl of Roche SYBR Green I Master mix containing dNTPs, Taq Polymerase and SYBR Green I (Roche Diagnostics, Laval, Quebec, Canada). $MgCl_2$ was added in the PCR reaction at a final concentration of 2.5mM. The total PCR reaction volume was 20µl.

2.5 RNA extraction

Total cerebellar RNA was extracted using the Qiagen RNeasy Mini Kit (P/N 74104) as per the supplier's protocol (Qiagen Inc. Canada, Mississauga, Ontario, Canada). The quantification and quality of the RNA was assessed using the spectrophotometer (Eppendorf BioPhotometer).

2.6 DNA Affymetrix Microarray analysis

Total cerebella RNA was extracted from 3 month old aged- and sex-matched transgenic animals as previously described. 200ul of RNA from each sample was concentrated by addition of 110µl of 5M sodium acetate (pH 5.2) and 495ul of 100% ethanol. The samples were placed at -20°C overnight to allow successful precipitation. Subsequently, the RNA was centrifuged at 14 000 RPM for 20 minutes at 4°C. The supernatant was discarded and the RNA pellet was washed with 500µl of 70% ethanol and were centrifuged at 14 000 RPM for 5 minutes at 4°C. The supernatant was discarded and the RNA pellet was allowed to air dry. 11µl of DEPC water was used to resuspend the RNA. To verify the integrity of the RNA prior to microarray analysis, samples were analysed using the Agilent Bioanalyzer (Agilent Technologies Canada Inc., Mississauga, Ontario,

Canada). A total of 20μg of total cerebellar RNA at a concentration of 2.0μg/μl was sent to Ottawa Genome Centre (The OHRI Gene Expression Facility, Ottawa, Ontario, Canada) for the microarray analysis. Cerebellar gene expression of nontransgenic, wt Ub-EGFP, K48R Ub-EGFP, K63R Ub-EGFP, and SCA1 mice (B05 line) were assessed using MG-U74A oligonucleotide array (Affymetrix, Santa Clara, CA, USA) containing 36 899 mouse genes and ESTs. Microarray data analysis was performed using GeneSpring 6.0 (Agilent Technologies Inc., Palo Alto, CA, USA) and Stratagene ArrayAssist 3.0 (La Jolla, CA, USA).

2.7 Quantitative RT-PCR analysis

A total of 1μg of template RNA from aged-matched nontransgenic, wt Ub-EGFP, K48R Ub-EGFP, B05 and B05 compound transgenic mice was used to prepare the first strand cDNA using M-MLV Reverse Transcriptase and Oligo$(dT)_{12\text{-}18}$ primers (Invitrogen Canada Inc, Burlington, Ontario, Canada) as per the supplier's protocol. The validation of the microarray results as well as the investigation of other target genes by RT-PCR was performed using the LightCycler® 1.5 instrument and SYBR Green I as the detection format (Roche Molecular Biochemicals, Mannheim, Germany).

The primer set used in the amplification of PKCγ was as follows: forward primer 5′-TTCTTCAAGCAGCCAAC-3′ and reverse primer 5′-TGTAGCTGTGCAGACG-3′. The following LightCycler® cycling conditions were used: (i) denaturation program (95 °C for 45 s); (ii) amplification and quantification programs were repeated 45 times (95 °C for 2 s; 58 °C for 10 s; 72 °C for 12 s with a single fluorescent measurement); (iii) melting curve program (70–99 °C continuous fluorescent measurement); and (iv) finally a cooling step to 40 °C.

The primer set used in the amplification of p300 was as follows: forward primer 5′-

CGCTTTGTCTACACCTGCAA-3′ and reverse primer 5′-TGCTGGTTGTTGCTCTCATC-3′. The following LightCycler® cycling conditions were used: (i) denaturation program (95 °C for 30 s); (ii) amplification and quantification programs were repeated 50 times (95 °C for 2 s; 55 °C for 10 s; 72 °C for 12 s with a single fluorescent measurement); (iii) melting curve program (70–99 °C continuous fluorescent measurement); and (iv) finally a cooling step to 40 °C.

The primer set used in the amplification of Calbindin was as follows: forward primer 5′-GACGGAAGTGGTTACCTGGA -3′ and reverse primer 5′-TTCCTCGCAGGACTTCAGTT-3′. The following LightCycler® cycling conditions were used: (i) denaturation program (95 °C for 20 s); (ii) amplification and quantification programs were repeated 35 times (95 °C for 1 s; 60 °C for 8 s; 72 °C for 12 s with a single fluorescent measurement); (iii) melting curve program (70–99 °C continuous fluorescent measurement); and (iv) finally a cooling step to 40 °C.

The primer set used in the amplification of EAAT4 was as follows: forward primer 5′-CAGATGCTGGTGTTACCCCT-3′ and reverse primer 5′AGGCCTCCACAAGGTTAGGT-3′. The following LightCycler® cycling conditions were used: (i) denaturation program (95 °C for 30 s); (ii) amplification and quantification programs were repeated 45 times (95 °C for 2 s; 60 °C for 8 s; 72 °C for 12 s with a single fluorescent measurement); (iii) melting curve program (70–99 °C continuous fluorescent measurement); and (iv) finally a cooling step to 40 °C.

The primer set used in the amplification of homer-3 was as follows: forward primer 5′-CTTACTATTTCGCACTCCCTTC-3′ and reverse primer 5′-ACTCAGTGTTTCCTGTCCC-3′. The following LightCycler® cycling conditions were used: (i) denaturation program (95 °C for 45 s); (ii) amplification and quantification

programs were repeated 45 times (95 °C for 2 s; 58 °C for 10 s; 72 °C for 12 s with a single fluorescent measurement); (iii) melting curve program (70–99 °C continuous fluorescent measurement); and (iv) finally a cooling step to 40 °C.

The primer set used in the amplification of CARP was as follows: forward primer 5′-CTTGCAGCGAAGGAGTTACC-3′ and reverse primer 5'-CACCAGTTCTACCCCCTTGA-3′. The following LightCycler® cycling conditions were used: (i) denaturation program (95 °C for 45 s); (ii) amplification and quantification programs were repeated 35 times (95 °C for 2 s; 58 °C for 10 s; 72 °C for 12 s with a single fluorescent measurement); (iii) melting curve program (70–99 °C continuous fluorescent measurement); and (iv) finally a cooling step to 40 °C.

The primer set used in the amplification of G-Substrate was as follows: forward primer 5′-GACTCTAAGATCTAGACGCCTC-3′ and reverse primer 5′-CCCCTCCCCATCTTTTATCC-3′. The following LightCycler® cycling conditions were used: (i) denaturation program (95 °C for 45 s); (ii) amplification and quantification programs were repeated 35 times (95 °C for 2 s; 58 °C for 10 s; 72 °C for 12 s with a single fluorescent measurement); (iii) melting curve program (70–99 °C continuous fluorescent measurement); and (iv) finally a cooling step to 40 °C.

The primer set used in the amplification of SERCA2 was as follows: forward primer 5′-CTGTGGAGACCCTTGGTTGT-3′ and reverse primer 5′-CAGAGCACAGATGGTGGCTA-3′. The following LightCycler® cycling conditions were used: (i) denaturation program (95 °C for 45 s); (ii) amplification and quantitation program repeated 35 times (95 °C for 2 s; 58 °C for 10 s; 72 °C for 12 s with a single fluorescent measurement); (iii) melting curve program (70–99 °C continuous fluorescent measurement); and (iv) finally a cooling step to 40 °C.

The primer set used in the amplification of IP3R1 was as follows: forward primer 5′-GTTCCAGAAACTGGCGAGAG-3′ and reverse primer 5′-CAGAGGCTCCTCTTTGGATG-3′. The following LightCycler® cycling conditions were used: (i) denaturation program (97 °C for 30 s); (ii) amplification and quantitation program repeated 45 times (95 °C for 2 s; 60 °C for 6 s; 72 °C for 12 s with a single fluorescent measurement); (iii) melting curve program (70–99 °C continuous fluorescent measurement); and (iv) finally a cooling step to 40 °C.

The primer set used in the amplification of ITPKC was as follows: forward primer 5′-CTGAGCGACAGTGAGAGCAG-3′ and reverse primer 5′-GCACCAGGCAGTAGTGTTCA-3′. The following LightCycler® cycling conditions were used: (i) denaturation program (95 °C for 45 s); (ii) amplification and quantitation program repeated 35 times (95 °C for 2 s; 58 °C for 10 s; 72 °C for 12 s with a single fluorescent measurement); (iii) melting curve program (70–99 °C continuous fluorescent measurement); and (iv) finally a cooling step to 40 °C.

The primer set used in the amplification of AMPA was as follows: forward primer 5′-TGTCAAAGTGGTGAGAGGCA -3′ and reverse primer 5′-ACAATAGTGGCTGCGGAAAC-3′. The following LightCycler® cycling conditions were used: (i) denaturation program (95 °C for 45 s); (ii) amplification and quantitation program repeated 45 times (95 °C for 2 s; 58 °C for 10 s; 72 °C for 12 s with a single fluorescent measurement); (iii) melting curve program (70–99 °C continuous fluorescent measurement); and (iv) finally a cooling step to 40 °C.

The primer set used in the amplification of the β-actin control gene was as follows: forward primer 5′-TTACTGCTCTGGCTCCTAG-3′ and reverse primer 5′-AAAGAAAGGGTGTAAAACG-3′.

PCR conditions were as follows: 4pmols of forward or reverse primer; 0.4µl of Taq Polymerase (Invitrogen Canada Inc, Burlington, Ontario, Canada); 1.6µl of dNTP (10mM); 0.4µl SYBR Green I ((1/10 000) Cambrex, Cambrex BioScience Rockland Inc, Rockland, ME, USA); 0.4µl BSA (25mg/ml (Sigma)); 4mM $MgCl_2$; and a total reaction volume of 20µl. The LightCycler® software package Version 5.3.2 was used to determine relative expression levels of the target gene (Roche Molecular Biochemicals, Mannheim, Germany). Quantification of all genes was extrapolated from a standard curve constructed from a serial dilution of control RNA. Fold changes in the various mouse lines were calculated relative to nontransgentic controls.

2.8 Northern blot analysis

RNA was extracted from the cerebella of 3 month old aged- and sex-matched nontransgenic, wt Ub-EGFP, K48R Ub-EGFP, B05 and B05 compound transgenic mice with the Qiagen RNeasy kit as previously described. 15µg of total RNA was denatured by heating at 65°C for 30 minutes and was separated on a 1% agarose-5% formaldyhyde gel. The migration and integrity of the RNA was confirmed by ethidium bromide staining for 15 minutes at room temperature. The RNA was transferred onto a Hybond N+ membrane overnight (Amersham Pharmacia Biotechnologies, Baie D'Urfé, Québec, Canada). Subsequently, it was incubated for 3 hours at 42°C in pre-hybridization solution containing 50% formamide, 20X SSPE, 50X Denhardt solution, 10% SDS and 250µg/ml denatured sperm DNA prior to the addition of the radiolabelled probe which consisted of a 2.7 Kb cDNA fragment encoding the non-expanded ataxin-1 protein (a gift from Huda Zoghbi, Baylor College of Medicine). The fragment was excised from the PGEMII backbone with EcoR1 restriction endonuclease and labelled with [α -32P] dCTP using a Megaprime DNA labelling kit from Amersham. The membrane was washed two

times for 15 minutes each at room temperature with buffer containing 2X SSC and 0.1% SDS, and then a final wash for 15 minutes with 0.2X SSC and 0.1% SDS at 65°C. The membrane was exposed on a phosphor screen and visualized with the phosphoimager (Amersham). As a loading control, the membrane was re-probed with a 1.1 Kb human β-actin c-DNA fragment excised from the Bluescript SK$^-$ backbone with EcoR1 restriction endonuclease (American Type Culture Collection, Manassas VA).

2.9 Protein extraction

The cerebella of nontransgenic and transgenic animals were excised as described previously. Tissue was homogenized in protein lysis buffer (20 mM Tris-HCl pH 7.5, 150mM NaCl, 1% Nonidet P-40 (Sigma, St. Louis, Missouri, USA), 0.5 mM EDTA, and 20% glycerol) containing the following protease and phosphates inhibitors: 1mM phenylmethylsulfonyl fluoride, 5 μg/mL leupeptin (Sigma), 2 μg/mL aprotinin (Sigma), 200 μM sodium Fluoride (NaF) and 200 μM sodium pyrophosphate (NaPPi). The homogenates were sonicated three times for 10 seconds each and placed on ice. The extracts were centrifuged at 14 000 RPM at 4°C for 30 minutes and the supernatants were recovered and pre-cleared by incubation with gamma bind sepharose beads (Amersham Pharmacia Biotech, Piscataway, NJ, USA) overnight at 4°C. The protein concentration of each sample was determined using the Bradford protein assay (Bio-Rad Laboratories Canada Inc., Mississauga, Ontario, Canada).

2.10 Western blot analysis

A total of 50μg of cerebellar protein extracts were resolved on an 8% SDS-polyacrylamide gel and electroblotted onto a hydrobond C nitrocellulose membrane (Amersham Pharmacia Biotech, Baie D'Urfé, Québec, Canada). The membranes were stained with Ponceau S (Sigma, St. Louis, Missouri, USA) prior to western blotting to

ensure complete transfer of proteins. Non specific binding was reduced by incubating membranes in 5% skim milk diluted in TBST (10 mM Tris-HCl (pH7.6), 150 mM NaCl and 1%Tween-20) overnight. The respective primary and secondary antibodies, which were also diluted in 5% skim milk in TBST, were applied on the membrane for 1 hour at room temperature. The membranes were then washed 3 times for 10 minutes with TBST prior to incubation with the appropriate secondary antibody. The proteins were visualized by the horseradish peroxidase method using the ECL kit purchased from Kirkegaard and Perry Laboratories Inc (Gaithersburg, Maryland, USA). Densitometry was performed in PhotoshopCS (Adobe System, San Jose, CA, USA). The values represent the mean intensity of pixels normalized to actin and expressed as the percentage of black (the raw scanned data were in the form of 256 shades of gray).

2.11 Antibodies for Western blot analysis

The mouse monoclonal 6xhis antibody was purchased from Qiagen (Qiagen Inc., Mississauga, Ontario, Canada). The rabbit polyclonal antibody raised against ubiquitin was purchased by DAKO (DakoCytomation Inc., Mississauga, Ontario, Canada). EGFP, RNA polymerase, and homer were detected with rabbit polyclonal antibodies purchased from Santa Cruz (Santa Cruz Biotechnologies Inc., Santa Cruz, CA). The rabbit polyclonal antibody used for the detection of PCAF was purchased from Upstate (Upstate Biotechnolgies, Chicago, IL, USA). The rabbit polyclonal PSD95 antibody was purchased from Zymed Laboratoreis (Zymed Laboratories Inc., South San Francisco, CA, USA).

2.12 Immunohistochemistry

Cerebella of nontransgenic and transgenic animals were excised and fixed in 10% phosphate-buffered formalin overnight at room temperature. They were then transferred

to 70% ethanol for a period of 24 hours prior to being paraffin-embedded and sectioned at a thickness of 5μm. Deparaffinized sections were heated in a solution of 10 mM sodium citrate (pH 6.0) in 700W microwave for 10 minutes. Endogenous peroxidase activity was blocked by incubating in methanol containing 3% hydrogen peroxide for 20 minutes. Sections were washed with 0.1 M PBS (pH 7.4) and incubated for 30 minutes with 1.5% normal goat serum (Santa Cruz Biotechnologies Inc., Santa Cruz, CA) to block nonspecific binding. Sections were then incubated overnight at 4°C with a rabbit polyclonal antibody raised against calbindin (Chemicon, Temecula, CA, USA). The reaction product was visualized by the Envision+ system (DakoCytomation Inc., Mississauga, Ontario, Canada). The number of Purkinje cells per 100μm was measured using the Zeiss software Axiovision 3.1 (Carl Zeiss, Thornwood, NY).

2.13 Behavioural analysis

Cohorts of six mice of each genotype were tested for motor performance on the rotating rod apparatus. They were placed on the rotating rod for three trials per day for four consecutive days. A period of several seconds before each trial without any acceleration of the rod was allocated to acclimatize the animal to the apparatus. The duration of the trials was approximately 6 minutes during which time the rod underwent linear acceleration in increments of 0.1 rpm/sec. Animals were scored for their latency to fall (in seconds) for each trial. Standard errors for the data were calculated using an algorithm in Excel (Microsoft Corporation, Redwood, WA, USA).

2.14 Cerebella neuronal cultures

Plastic culture dish (diameter of 35mm; Falcon 3001) were coated by placing 300ul of poly-L-Ornithine (PLO; 500ug/ml) overnight. Before use, dishes were rinsed with purified water three times and completely dried. The stock solution for seeding and

culture media was a 1:1 mixture of Dulbecco's modified Eagle medium and F-12 nutrients (DFM; Gibco 12400), supplemented with Purescine (100uM), Na_2SeO_3 (30nM), L-glutamine (1.4mM), and gentamicin (10ug/ml); pH was adjusted to 7.2 with NaOH. E 18 embryos were removed by caesarean-section from various mouse strains and anaesthetized with diethylether. The embryos were sacrificed by decapitation, and their cerebella were dissected and kept in 10 ml of ice-cold Ca^{2+} - and Mg^{2+} -free Hank's balanced salt solution (Gibco 21250) containing fentamicin (10ug/ml) (HBSS). The cerebella were processed in a 15-ml plastic tube (Falcon 2096). To change solution, we centrifuged the tube at 1000 rpm, 4°C for 1-3 min, aspirated the supernatant, and then poured new solution into the tube. The cerebella were washed with 10ml HBSS once and digested in 2.5ml TrypLE Express (Invitrogen) at 33°C for 13-15 min. The dissected cerebella were rinsed with 10ml of HBSS twice. In 2ml of HBSS supplemented with $MgSO_4$ -$7H_2O$ (12 mM) and DNase I (5U.ml; 776 785, Boehringer), the cerebella were gently triturated with the same pipette to which was attached a plastic tip until they became invisible. Five millilitres of HBSS was added to the cell suspension and the tube was centrifuged at 1200 rpm, 4°C for 5 min. After removal of supernatant, the density of dissociated cells was adjusted to 5 X 10^6 cell/ml with DFM stock solution supplemented with foetal bovine serum (BSA)(10% v/v; 29-167-54, ICN). A 90-ul drop of the resultant seeding medium was gently placed on the coated area of a culture dish. Culture medium was added to each dish. After 3-h incubation in the CO_2 incubator, 1 ml of culture medium was added to each dish. Culture medium was prepared before use by supplementing the DFM stock solution with transferring (200ug.ml), progesterone (40nM) insulin (20 ug/ml), and tri-iodothyronine (0.5 ng/ml), which is reported to be important for PN differentiation such as dendritic branching (see Lindholm et al., 1993). The cells

were maintained in the incubator and fed once a week by replacing half of the old medium with cytosine arabinoside (4uM) and BSA (100ug/ml).

Chapter 3

Results

3.1 Generation of novel ubiquitin transgenic mice

Although readily detected in its monomeric form, ubiquitin is never expressed in such a way in cells but rather as a precursor pro-protein either as a tandem repeat of multiple ubiquitin moieties or as a fusion with ribosomal subunits. These ubiquitin fusion proteins are processed during translation by ubiquitin carboxyterminal hydrolases (UcHs) or ubiquitin specific proteases (DUBs) to yield ubiquitin monomers that can be covalently attached to protein substrates. This property of ubiquitin processing was exploited to generate expression constructs encoding in frame fusions between an RGS-6xHis epitope tagged ubiquitin with the enhanced green fluorescent protein (hereafter referred to as EGFP) under the control of the strong UbC promoter (a schematic representation of the expression cassette is depicted in Figure 4), The strategy employed predicts that, much like endogenous ubiquitin fusion proteins, linear fusions of ubiquitin with EGFP would be processed by endogenous enzymes possessing ubiquitin processing activity to yield functional ubiquitin moieties and EGFP that serves as a proxy for detection. An image of dissected brains and testis from a wt Ub-EGFP expressing transgenic mouse viewed by light and fluorescent microscopy is shown in Figure 5 to demonstrates the ubiquitous expression of the transgene in these organs. The functionality of the ubiquitin expression constructs has been previously tested in cultured mammalian cells (Tsirigotis et al., 2001a) and in vivo (Tsirigotis et al., 2001b). A western blot of total brain extracts prepared from nontransgenic, wild-type, K48R and K63R mice probed with antibodies raised against EGFP, ubiquitin and the 6xhis epitope respectively is shown in Figure 6 to demonstrate the expected protein species when efficient processing occurs and the incorporation of

Figure 4. General design of the ubiquitin expression constructs

The human ubiquitin C promoter (UbC) was used to drive the expression of the hexahistidine-tagged human ubiquitin (Ub) fused in frame to the enhanced Green Fluorescent protein (EGFP). The simian virus 40 polyadenylation signal (pA) was placed downstream. The arrow shows the Ub-EGFP cleavage site. Cleavage of EGFP serves as a proxy for detection of the transgene. The hexahistidine-tag serves as an epitope for detection of ubiquitinated substrates that have incorporated transgene-derived ubiquitin. The most characterized polyubiquitin chains in which ubiquitin can participate are indicated and consist of chains linked through lysine 48 (resulting in a 'zig-zag' conformation) or lysine 63 (resulting in a linear chain). DUBs: Deubiquitinating enzymes. S: protein substrate.

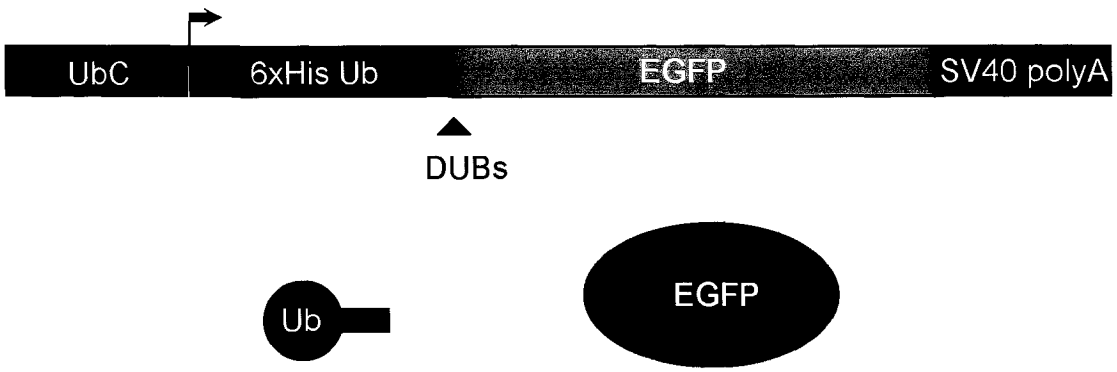

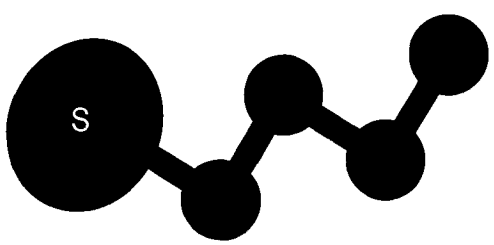

K48 linked chains

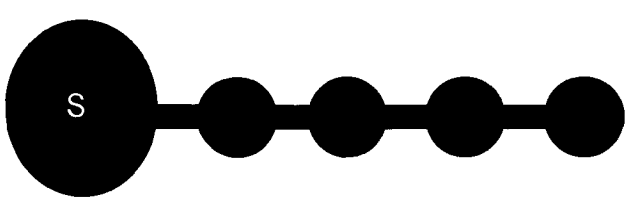

K63 linked chains

M,Tsirigotis, 2005

Figure 5. In vivo expression of the EGFP marker in transgenic brains

Phase contrast microscopy of A) morula-stage embryo from a heterozygous X wild-type cross, B) newborn littermates from a heterozygous X wild-type cross, and C) dissected brains from a nontransgenic mouse (left) and its transgenic littermate (right). When viewed under fluorescent light the transgenic mice were found to be intensely fluorescent (lower panel).

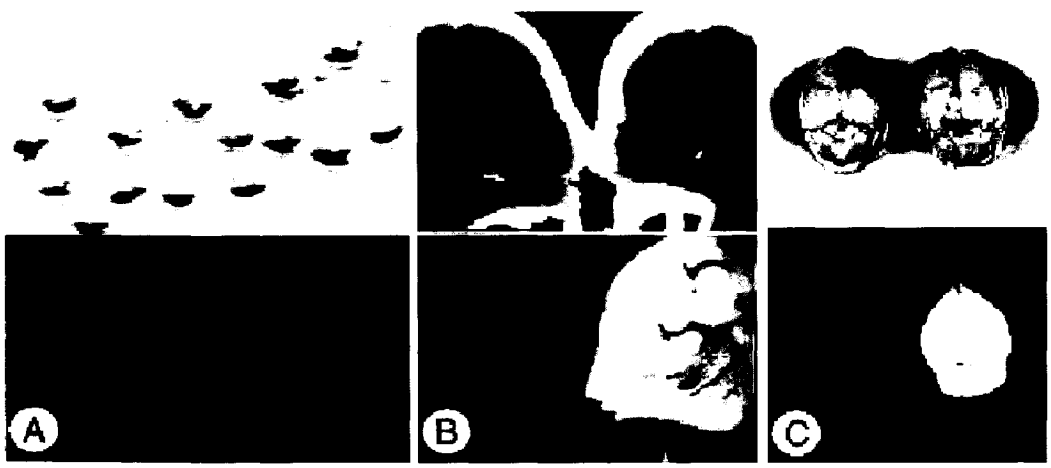

Tsirigotis et al, 2001

Figure 6. In vivo processing and conjugation of transgene-derived ubiquitin

A) Transgene-derived ubiquitin was detected using an antibody specific for the 6xHis epitope tag. The presence of monomeric ubiquitin (solid arrow) confirmed that the Ub-EGFP fusion was efficiently processed. This species was absent in lysates from nontransgenic animals. B) Analysis of total ubiquitin levels in brain lysates. Over expression of transgene derived ubiquitin did not increase the levels of ubiquitin (solid arrow) or respective conjugates (ubiquitin smear). C) Western blot analysis with an EGFP-specific antibody. The antibody detected the processed form of the EGFP marker (asterisk) in lysates of transgenic mice that was absent in nontransgenic control brain extract. EGFP levels served as an indicator of transgene expression; expression appeared to be similar in the ubiquitin mutants. A slight decrease was noted in with wild type ubiquitin brain lysates. β-actin was used as a loading control (arrowhead).

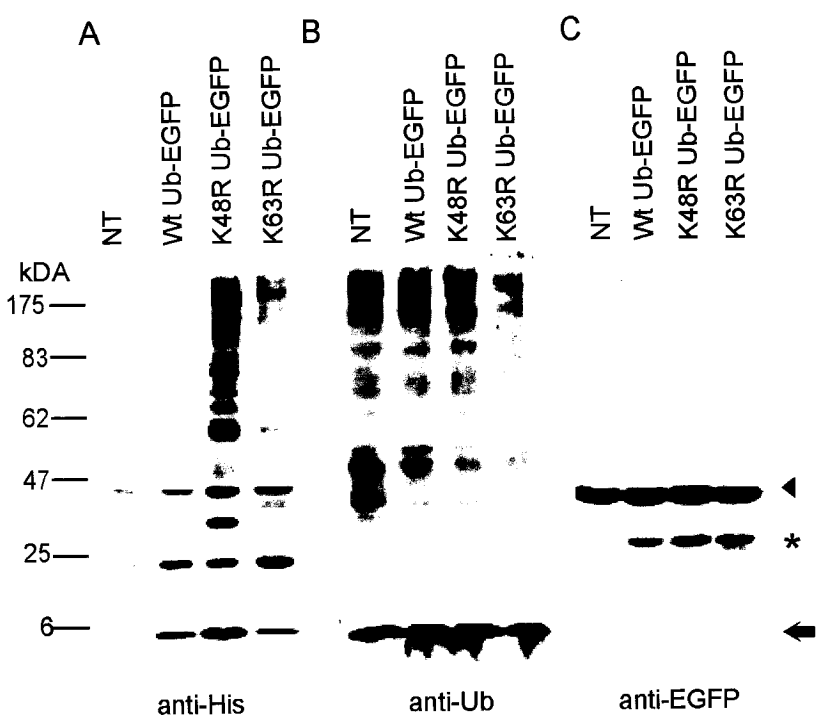

Zhang et al, 2003

transgene-derived ubiquitin in higher order conjugates. A single band representing the processed EGFP marker (rather than the fusion protein) was detected when the membrane was probed with an EGFP-specific antibody in each of the lysates derived from the transgenic brains. EGFP protein levels were also used to assess the relative levels of transgene expression which did not appear to differ significantly between the various ubiquitin transgenics. The processed EGFP marker was absent in lysates from nontransgenic control animals. The analysis of the same extracts by western blotting with an antibody raised against the 6xHis epitope revealed the presence of a protein species with a molecular mass consistent with monomeric ubiquitin as well as higher order ubiquitylated conjugates. These species were absent in nontransgenic control brain lysates. Re-probing the membrane with an ubiquitin-specific antibody confirmed the presence of ubiquitin in these higher order molecular weight species and revealed that the total levels of ubiquitin (endogenous and transgene derived) did not differ significantly in the transgenic strains suggesting that the presence of the transgenes did not result in the upregulation of the stress-inducible endogenous ubiquitin genes.

3.2 Establishment of a genotyping strategy using Real-Time PCR

Much of the research in the current thesis relies on accurate genotyping. An early objective was to determine if conditions could be identified that could discriminate between ubiquitin transgenes differing at a single codon. In order for the genotyping strategy to be informative, it was necessary to design primers that would solely amplify transgene-derived ubiquitin (rather than endogenous ubiquitin genes) and capable of discriminating between the wild-type and mutated sequence. To accomplish this, primers

that recognized sequences in ubiquitin corresponding to wild type K48, mutant K48R, wild type K63, and mutant K63R were designed in conjunction with a reverse primer that recognized a DNA sequence within the EGFP reporter (Figure 7). All primers were designed to amplify a 240bp or 210bp product, at position 48 or 63 respectively, and had a melting temperature of ~67°C (Table 1). Each template DNA was assayed in 4 separate PCR reactions using the primer sets described above. Figure 8a represents a LightCycler graph showing the amplification of DNA extracted from a wt Ub-EGFP mouse with the wild type K48 and wild type K63 primer sets along with the gel analysis of the product identifying the sample as DNA extracted from a wild type Ub-EGFP mouse. Figure 8b shows the amplification of mutant K48R and wild type 63, along with the gel analysis, identifying the sample as K48R. Finally, primer sets from wild type 48 and mutant K63R are seen in the amplification curve along with the accompanying gel analysis, identifying the sample as DNA extracted from K63R Ub-EGFP mice (Figure 8c).

The combinatorial analysis of successful amplification from each primer set (at positions 48 or 63) was used as a determinant of the genotype of the animal. The results of this PCR based genotyping strategy along with the ethidium bromide staining of the agarose gels are shown in Figure 8. Primer sets corresponding to wild type K48 and wild type K63 (but not the mutant K48R or mutant K63R) amplified products at the expected sizes from genomic DNA extracted from a wild type Ub-EGFP mouse. In contrast, DNA extracts from a K48R Ub-EGFP or K63R Ub-EGFP mouse only amplify with primer sets corresponding to mutant K48R and wild type K63 or wild type 48 and K63R respectively. No bands were observed in amplification reactions where nontransgenic DNA or water (used as negative control) was utilized as the template.

Figure 7. General design of the ubiquitin genotyping primers

Primers were designed to amplify a 240bp or 210bp fragment. The primers recognized the region of ubiquitin in which the mutation has been introduced and the sequence of the primer was either wild-type or mutant at the K48 or K63 sites. The expected size fragments if successful amplification occurs are also indicated.

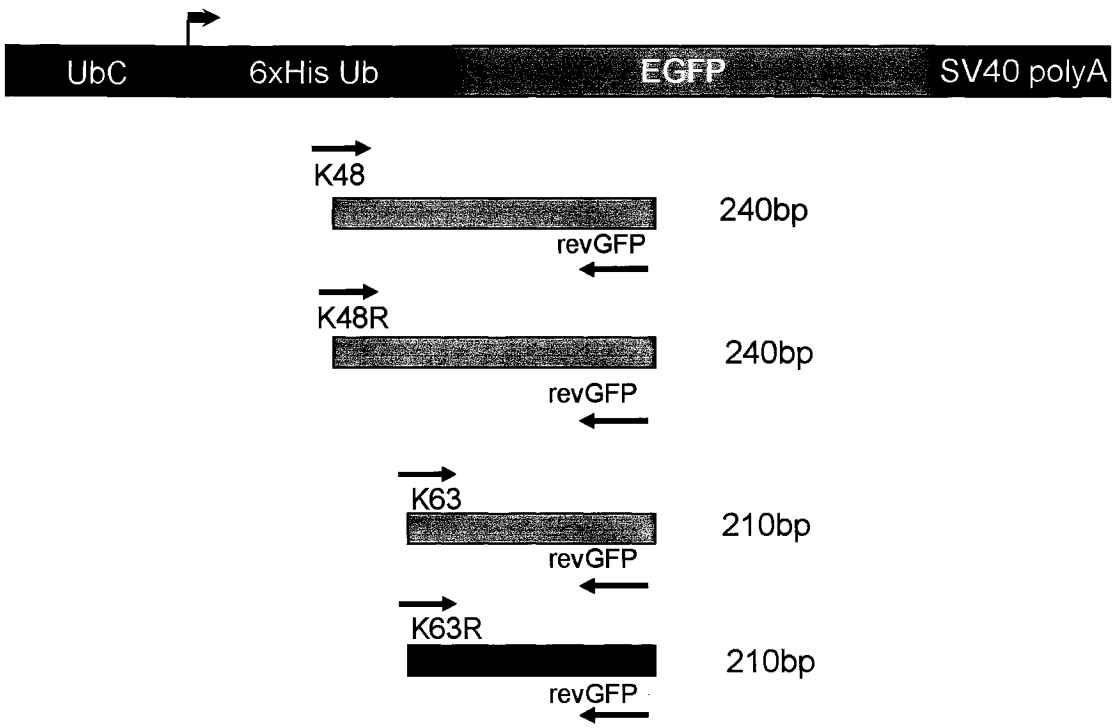
UbC
6xHis Ub
EGFP
SV40 polyA
K48
240bp
revGFP
K48R
240bp
revGFP
K63
210bp
revGFP
K63R
210bp
revGFP

Table 1. Sequences of the ubiquitin primers used in the genotyping

A total of 4 forward primers and 1 reverse primer were used for the genotyping strategy. Each primer was designed to have similar melting temperatures to avoid bias during the initial annealing step. This was achieved by adjusting the length and the percentage of G-C content of each primer. The trinucleotide corresponding to the respective point mutation is highlighted in yellow.

Oligo Name	Length	Melting temperature (C°)	Sequence(5′-3′)
K48	18	67.9	GCAGGCAAGCAGCTGGAA
K48R	16	68.5	AGGCCGGCAGCTGGAA
K63	21	64.4	ATCCAGAAAGAGTCGACCCTG
K63R	18	66.4	AACATCCAGCGGGAGTCG
RevGFP	18	67.5	CTTGCCGGTGGTGCAGAT

Figure 8. Genotyping novel ubiquitin transgenic mice using the LightCycler®

Real-Time amplification curves showing changes in fluorescence in relation to PCR cycles and the respective gel analysis of the PCR products. Amplification of A) DNA from a wild type Ub-EGFP mouse showing the expected size fragment of 210 and 240bp in reactions where K63 and K48 primers were used respectively. B) DNA extracted from a K48R Ub-EGFP mouse. PCR products were observed in reactions where K48R and K63 primers were used. C) DNA derived from a K63R Ub-EGFP mouse only amplified in reactions where K63R or K48 primers were utilized.

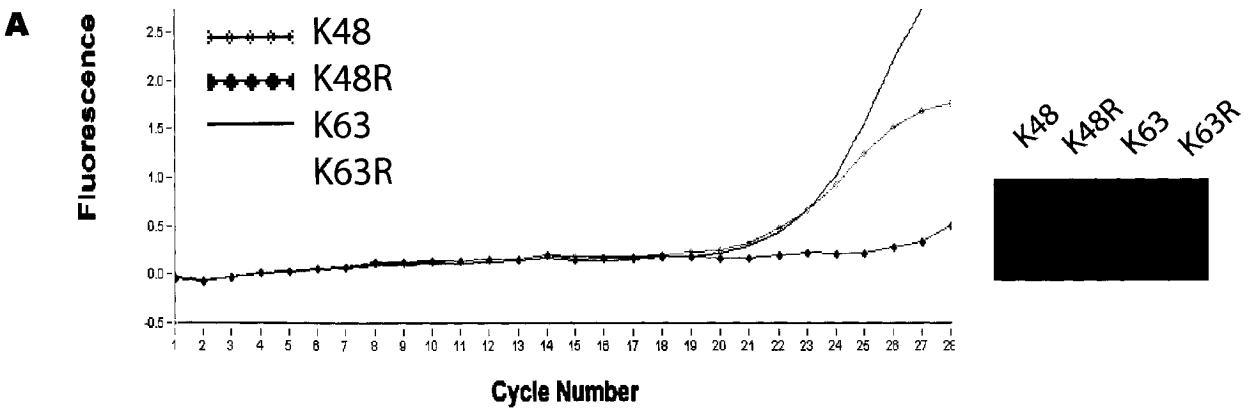
A
Fluorescence
K48
K48R
K63
K63R
Cycle Number
K48
K48R
K63
K63R

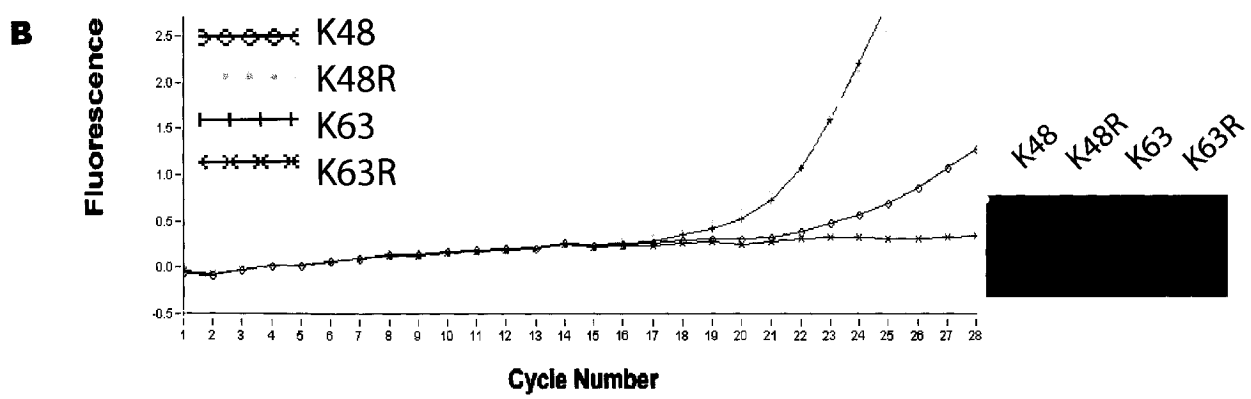
B
Fluorescence
K48
K48R
K63
K63R
Cycle Number
K48
K48R
K63
K63R

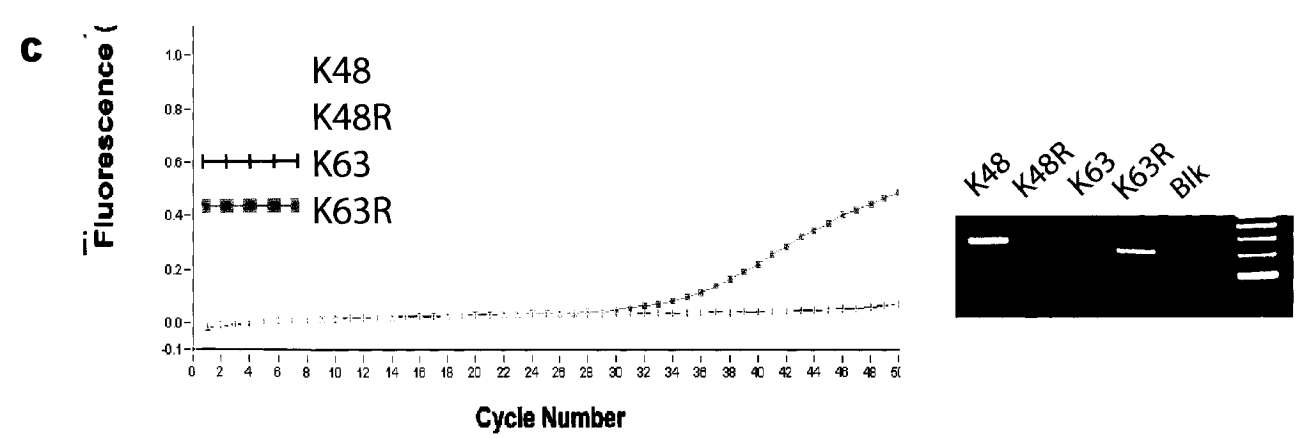
C
Fluorescence
K48
K48R
K63
K63R
Cycle Number
K48
K48R
K63
K63R
Blk

To test the efficacy of this genotyping strategy, an unbiased blind test with DNA extracted from all the different genotypes were randomized, unlabelled and subjected to genotyping analysis as described above. The results are summarized in Table 2 that indicates that 5 out of 8 samples were correctly identified. These samples consisted of a water, nontransgenic, wild type Ub-GFP, K48R, and K63R. However, intentionally contaminated samples consisting of 1) a mixture of 2 different DNA samples (wt Ub-EGFP and K48R), 2) all 3 genotypes mixed together, and 3) a nontrangenic sample that was spiked with K48R DNA were not correctly identified.

3.3 Delayed spinocerebellar ataxia in transgenic mice expressing mutant ubiquitin

The presence of ubiquitylated inclusions have long been a hallmark of neurodegenerative disorders. It remains unclear whether the presence of ubiquitylated deposits reflects the inability of the ubiquitin-proteasome pathway to successfully clear misfolded proteins and contribute to the exacerbation of the disease. If the clearance of misfolded proteins is limiting in disease, it is predicted that introducing a K48R chain-terminating variant of ubiquitin in the B05 background would exacerbate the phenotype by serving to stabilize the toxic protein (ataxin-1 has been shown to be subject to ubiquitin-dependent degradation (Cummings et al., 1998)). To test this hypothesis, compound transgenics were created by crossing a well characterized mouse model of spinocerebellar ataxia type 1 (strain B05 with a pathological expansion of 82 glutamine repeats within the gene product Ataxin-1) with each of the three ubiquitin transgenics (wild type, K48R, or K63R). As a control, the ubiquitin transgenics were also bred with strain A02 which contains a non-pathological expansion of 30 glutamines. Contrary to B05 mice, the A02 strain is asymptomatic.

Table 2. Summary of the validation of the genotyping strategy

Summary table indicating the efficacy of the genotyping strategy as tested in unlabelled samples. Out of the 8 unknown samples 5 were correctly identified and consisted of samples 2, 3, 4, 6, and 8. The 3 samples that were incorrectly identified were sample 1, 5 and 7 which consisted of a mixture of wt Ub-EGFP and K48R DNA, DNA from all three transgenics strains and DNA of a nontransgenic control spiked with DNA from a K48R transgenic, respectively.

Sample number	PCR result	Correct Identification?	Actual Sample
1.	K48R	no	1/2 (UbEGFP + K48R)
2.	K63R	yes	K63R
3.	K48R	yes	K48R
4.	UbEGFP	yes	UbEGFP
5.	K63R	no	All 3 transgenes
6.	NT	yes	NT
7.	NT	no	NT spiked with K48R
8.	Blk	yes	Blk

A primary feature in SCA1 is the progressive loss of cerebellar Purkinje neurons involved in motor coordination. It has been previously demonstrated that in B05 but not in A02 mice there is a progressive loss in these neurons eventually resulting in a complete disappearance of the population. Therefore, examination of the anatomical structure of the cerebellum was performed as an indicator of the progression or severity of the disease in each compound transgenic. Sections were stained with calbindin (a Purkinje-specific marker) and examined microscopically for several time points up to 8 months. As previously reported, pronounced morphological alterations of Purkinje neurons including aberrant dendritic morphology, unusual orientation or ectopic localization within the granular or molecular cell layers began to be visualized in 3-month old B05 mice. These morphological alterations appeared less pronounced in B05x K48R mice and in B05 x wt Ub mice (Figure 9). Genetic crosses between B05 and K63R appeared similar to B05 (Tsirigotis et al., 2005 in press).

3.4 K48R mutant ubiquitin improves coordination in SCA1 mice

The anatomical data suggested that the deterioration of Purkinje cells was delayed in mice expressing K48R mutant ubiquitin as opposed to the other ubiquitin isoforms in the presence of the expanded polyglutamine protein. To investigate whether this translated to an enhanced coordination, motor performance was assessed using the rotating rod apparatus in simple and compound transgenic mice at the 3 month time point. There was a pronounced amelioration of motor performance in mice expressing K48R mutant ubiquitin as opposed to wild type and K63R Ub ubiquitin in the presence of the expanded polyglutamine repeat (Figure 10). However, these differences in performance were

Figure 9. Purkinje cell morphology in mice at 3 months of age.

Calbindin-expressing Purkinje neurons (reddish brown) and nuclei (purple) were visualized by immunohistochemistry. A) Nontransgenic control cerebellum, showing orderly Purkinje cell layer with some dendritic processes visible. B) Heterozygous A02 cerebellum, similar in appearance to the nontransgenic control. C) Heterozygous B05 cerebellum, showing pathological Purkinje morphology, including vesicle formation, aberrant orientation and ectopic localization of Purkinje neurons within the molecular layer. D) Cerebellum from B05 x Wt Ub cross, with evidence of vesicles. E) Cerebellum from B05 x K63R Ub cross, with pathological indicators as in B05 heterozygote. F) Cerebellum from B05 x K48R Ub cross, showing some evidence of vesiculation of Purkinje neurons and altered orientation, but less severe pathology than is evident in B05 heterozygous sections (C). Bar =100μM.

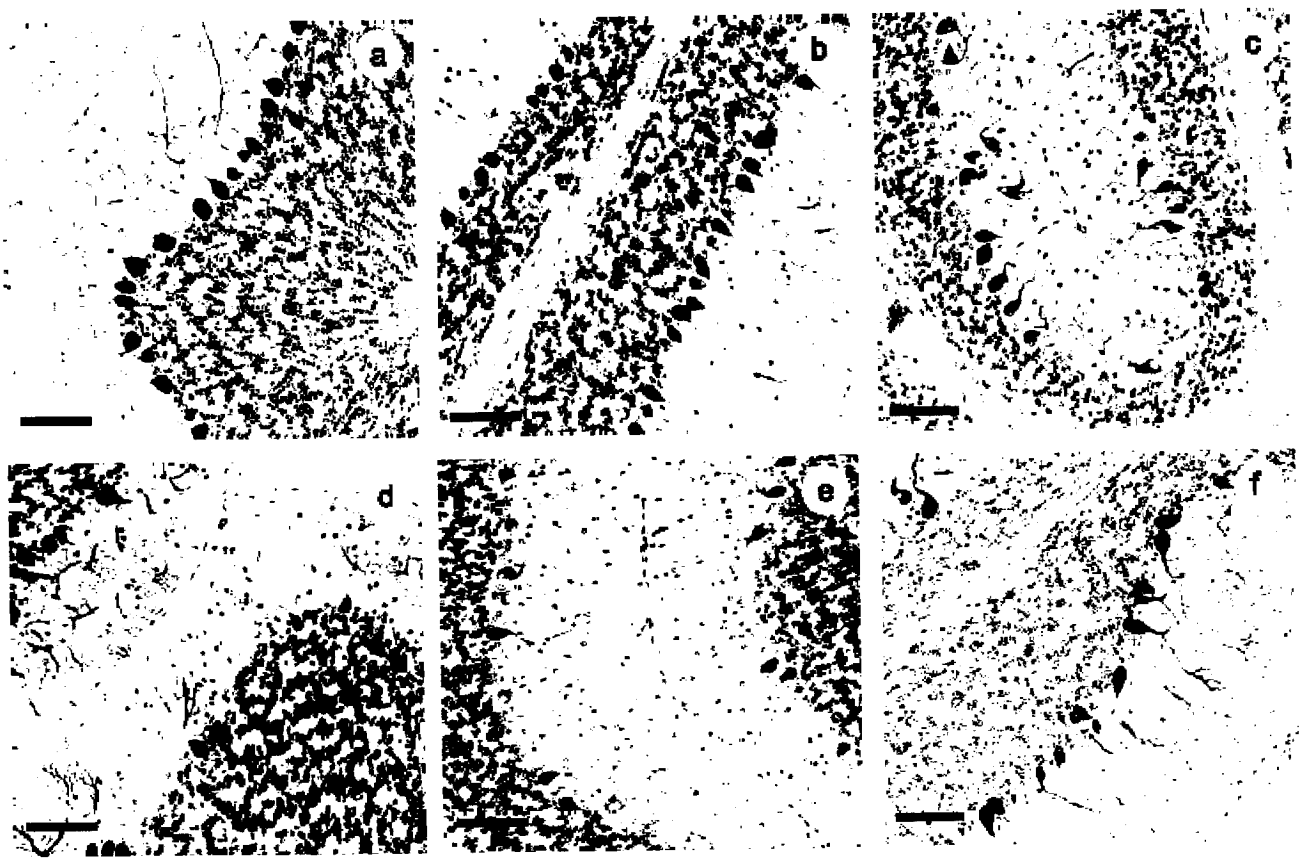
a
b
c
d
e
f

Figure 10. Assessment of motor skills using the rotating rod apparatus

B05 x K48R compound heterozygous mice showed performance similar to that of nontransgenic control animals at 3 months of age, whereas other genetic crosses fared no better than B05 heterozygous mice. Bars represent standard error of the mean.

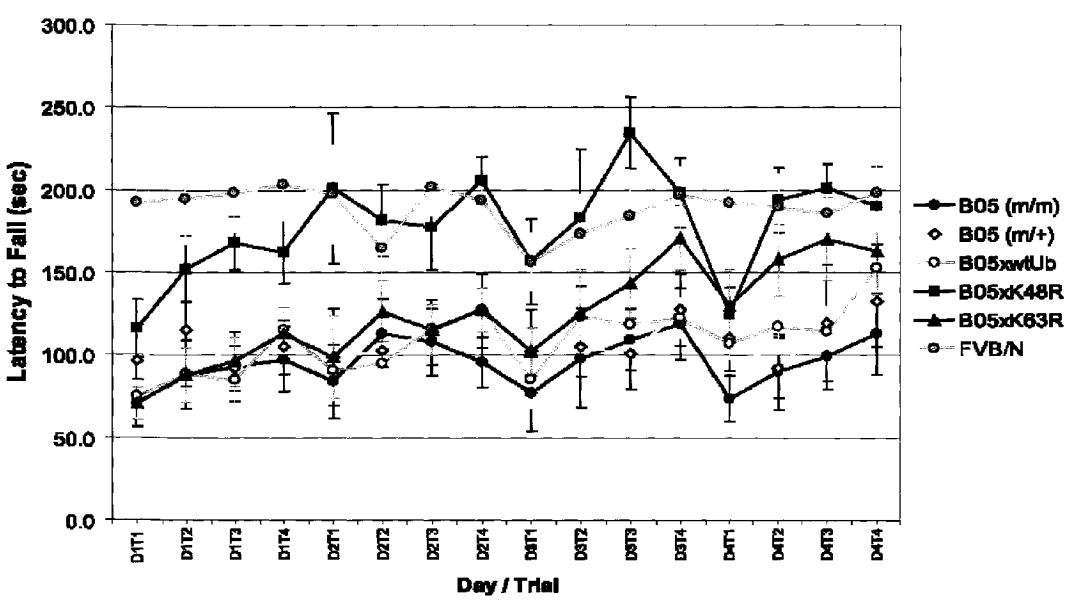
300.0
250.0
200.0
150.0
100.0
50.0
0.0
Latency to Fall (sec)
D1T1
D1T2
D1T3
D1T4
D2T1
D2T2
D2T3
D2T4
D3T1
D3T2
D3T3
D3T4
D4T1
D4T2
D4T3
D4T4
Day / Trial
B05 (m/m)
B05 (m/+)
B05xwtUb
B05xK48R
B05xK63R
FVB/N

transient in nature and became undetectable at later time points. As expected, there were no observable differences in the performance of the A02 mice and respective crosses when compared to nontransgenic controls.

3.5 Dysregulated transcription in SCA1 mice

A feature of SCA1 (much like other polyglutamine diseases) is the well documented loss of transcription of neuronal genes (Lin et al., 2000) through a mechanism involving the sequestration of transcription factors by the expanded protein. It was speculated that a reprogramming of transcription may account for the delay in the phenotype in B05 x K48R and to assess potential transcriptional changes in disease progression of SCA1, we profiled cerebellar RNA of nontransgenic, wt Ub-EGFP, K48R Ub-EGFP, K63R Ub-EGFP and SCA1 mice (B05 line) at 3-month of age by independently hybridizing each sample to a Affymetirx microarray. A global view of gene expression using the microarray analysis software GeneSpring 6.0 (Agilent Technologies Inc., Palo Alto, CA, USA) is shown in Figure 11. Consistent with published literature, the analysis revealed a number of dysregulated genes (that were either up- or down-regulated) that have been previously found to be altered in the course of SCA1 (Table 3). Comparison of mRNA profiles of the ubiquitin transgenics revealed the presence of certain altered transcripts but the differences in expression were not as large as they were found to be in B05 mice. Gene clustering of similarly expressed genes using a different microarray software (Stratagene ArrayAssist 3.0) revealed a decrease in a number of genes directly involved in glutamate signalling in B05 animals. Amongst these dysregulated genes were inositol 1,4,5-trisphosphate receptor 1 (IP3R1), G-substrate, phosphatidylinositol (4,5) bisphosphate 5-phosphatase, Calbindin, gamma-aminobutyric

Figure 11. Summary of gene expression in cerebella of 3 month old mice

Microarray analysis using GeneSpring 6.0 revealed a number of changes in gene expression in B05 animals at 3 months of age. Each line in the graph represents the expression level of a particular gene. Genes within the upper quadrant are up-regulated whereas genes in the lower quadrant are downregulated. The X axis represents the various transgenic strains. The log normalized signal intensity is represented on the y-axis.

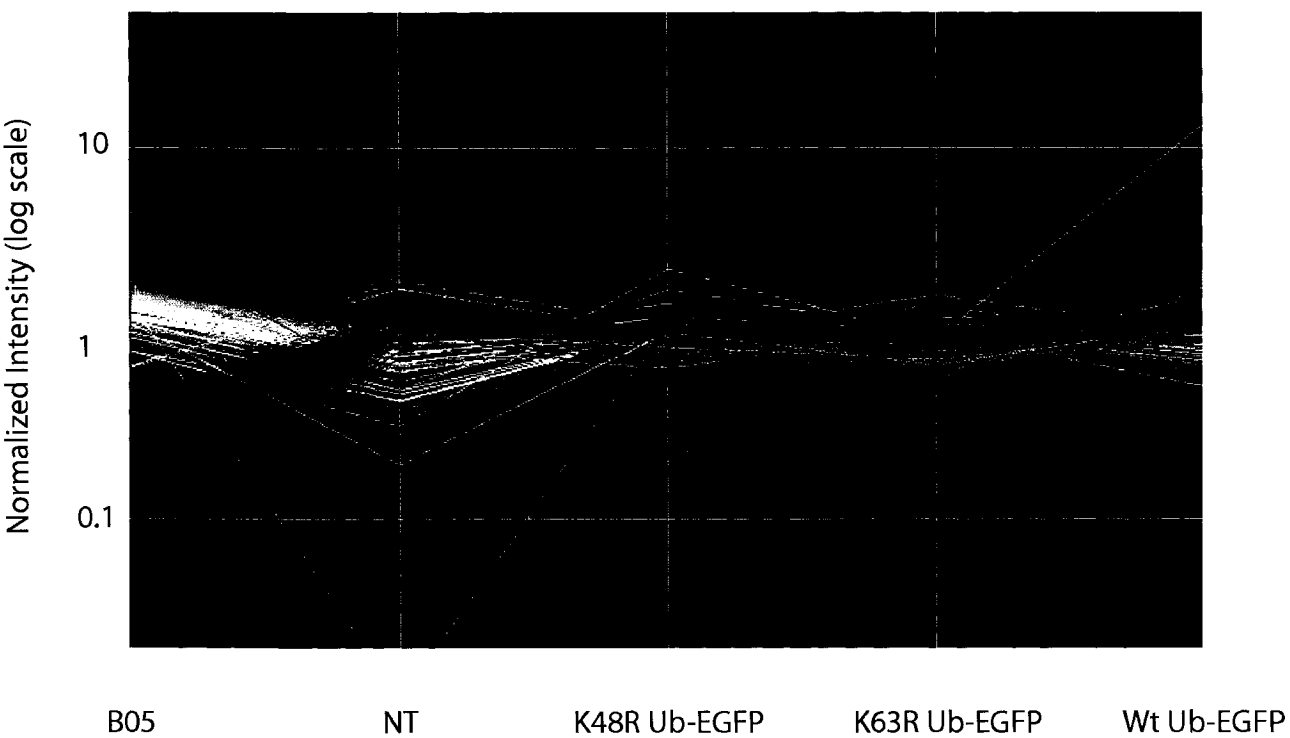
Normalized Intensity (log scale)
10
1
0.1
B05
NT
K48R Ub-EGFP
K63R Ub-EGFP
Wt Ub-EGFP

Table 3. Summary of altered genes in B05 mice

Gene clustering analysis using Stratagene ArrayAssist 3.0 revealed a striking dysregulation of many glutamate and calcium regulatory genes in B05 mice. Numbers represent logarithmic fold changes relative to nontransgenic controls.

ubGFP	K48R	K63R	BO5	NT	
-0.67	0.22	-0.05	-5.13	0.00	inositol 1,4,5-triphosphate receptor 1
-0.75	-0.67	-0.75	-4.43	0.00	G substrate
0.01	0.60	0.43	-4.32	0.00	glutamate receptor, ionotropic, N-methyl D-asparate-associated protein 1 (glutamate
-0.37	-0.39	-0.42	-3.49	0.00	phosphatidylinositol (4,5) bisphosphate 5-phosphatase, A
-0.86	-0.41	-0.47	-3.48	0.00	calbindin-28K
-0.05	0.18	0.00	-2.91	0.00	glutamate receptor, ionotropic, AMPA1 (alpha 1)
-0.90	-0.22	-0.26	-2.79	0.00	inositol polyphosphate-5-phosphatase A
-0.77	0.08	-0.31	-2.70	0.00	inositol 1,4,5-triphosphate receptor 1
-0.24	0.09	-0.09	-2.57	0.00	gamma-aminobutyric acid (GABA-A) receptor, subunit alpha 1
0.19	0.80	0.58	-2.49	0.00	calbindin 2
-0.12	0.11	-0.01	-2.35	0.00	glutamate receptor, ionotropic, delta 2
0.07	0.23	-0.06	-1.97	0.00	calcium/calmodulin-dependent protein kinase II, delta
0.01	0.49	0.28	-1.96	0.00	glutamate receptor, ionotropic, N-methyl D-asparate-associated protein 1 (glutamate
0.01	-0.04	0.00	-1.66	0.00	glutamate receptor, ionotropic, NMDA1 (zeta 1)
-0.14	-0.31	-0.31	-1.13	0.00	glutamate receptor, ionotropic, AMPA4 (alpha 4)

acid (GABA-A) receptor, calcium/calmodulin-dependent protein kinase II, and various glutamate receptors all of which have been previously shown to be affected in SCA1(Serra et al., 2004).

3.6 Gene reprogramming in mouse model of SCA1 by mutant K48R ubiquitin

Having established that B05 mice have an altered gene expression profile we sought to determine if the loss of these genes is restored in the genetic crosses and if such a restoration of transcription may account for the amelioration of the phenotype. To confirm the findings of the Affymetrix microarray, selected target genes were validated by Real-Time PCR using the Roche LightCycler®. A list of the chosen genes is shown in Table 3. To investigate whether there was an amelioration of gene transcription in the genetic crosses, the gene expression levels were analysed by quatitative RT-PCR. Expression levels were extrapolated from a standard curve constructed from a serial dilution of control RNA (Figure 12). Fold changes in the various mouse lines were calculated relative to nontransgenic controls. In agreement with the microarray screen, the analysis of the Real-Time PCR data revealed that many target genes were indeed altered in B05 mice (Figure 13 and 14). The analysis revealed that many of the genes dysregulated in both the B05 and B05 x wtUb animals were partially rescued in the B05 x K48R transgenic mice suggesting that the protective effects may be a result of gene reprogramming. The genes that were partially restored in B05 x K48R crosses included: the calcium binding protein Calbindin, carbonic anhydrase-related protein CARP, G-substrate (involved in the internalization of AMPA receptors), Inositol 1,4,5-trisphosphate receptor (IP3R), inositol 1,4,5-trisphosphate 3-kinase C (ITPKC), and PKCγ (Figure 13) whereas AMPA, EAAT4, SERCA2 and homer remained

Figure 12. Generation of a standard curve for quantitative RT-PCR

Screen capture of Real-Time PCR using the LightCycler® software package Version 5.3.2. A representation of a standard curve constructed from serial dilution of a control cDNA sample. The curve was generated by plotting the C_t values for each diluted sample against its concentration resulting in a curve with a correlation efficiency that equals to 1 (r= -1.00). The expression levels were extrapolated from the standard curves and were compared to nontransgenic controls.

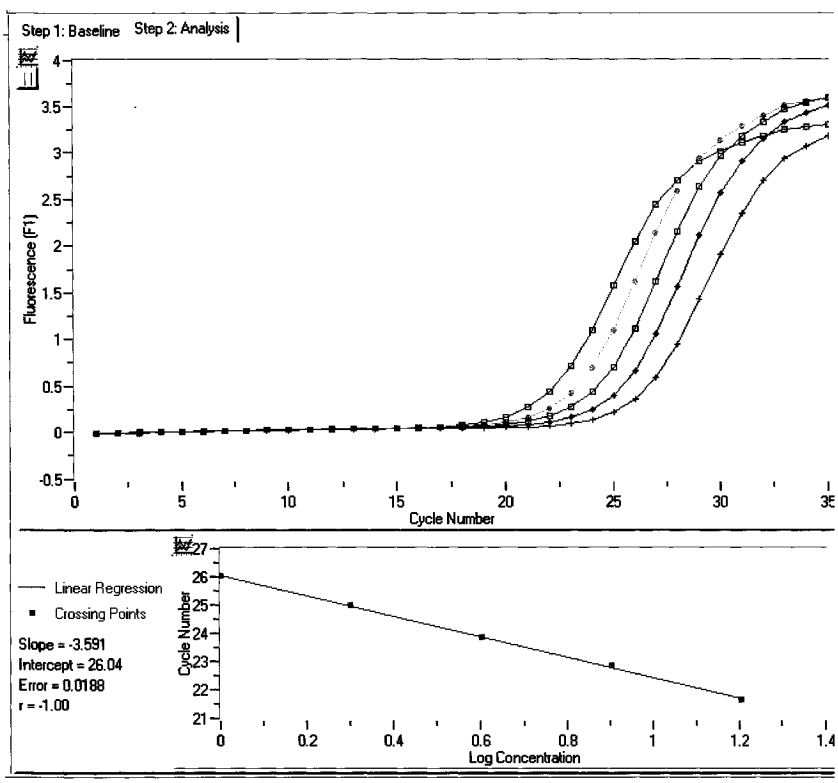
Step 1: Baseline
Step 2: Analysis
Fluorescence (F1)
Cycle Number
Linear Regression
Crossing Points
Slope = -3.591
Intercept = 26.04
Error = 0.0188
r = -1.00
Cycle Number
Log Concentration

Figure 13. Restoration of genes by K48R mutant ubiquitin

Comparative quantitative RT-PCR analysis in B05 and B05 crosses. A) Amplification curves showing changes in fluorescence versus PCR cycle for the PKCγ gene. A delay in DNA amplification was most striking in the B05 animals (green line) followed by B05 x Wt (purple) when compared to nontransgenic control DNA. DNA extracted from B05 x K48R animals (red) amplified at an early time than both B05 and the B05 x WtUb cross but not as quickly as the nontransgenic control (light green). No difference was observed in the straight ubiquitin transgenics. Wt Ub-EGFP (aqua) and K48R Ub-EGFP (gray). B) Bar graph representation of (A) showing the restoration of gene transcription of the PKC gamma gene in the B05 crosses. This pattern of gene expression was also consistently observed for C) the inositol 1,4,5-trisphosphate receptor (IP3R) gene, D) the inositol 1,4,5-trisphosphate 3-kinase C (ITPKC) gene, E) G-substrate gene, and F) Carbonic anhydrase-related protein (CARP) gene. Graph legends depicting B05 (black), B05 x Wt (blue), and B05 x K48R (red).

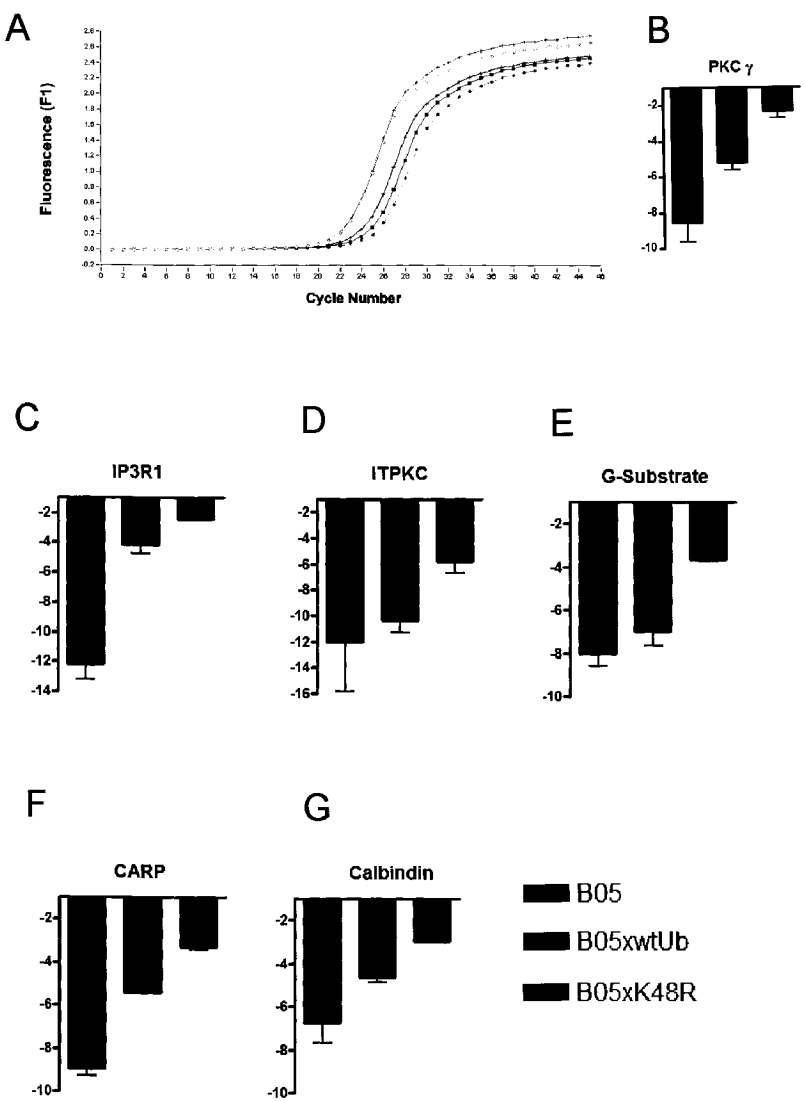
A
Fluorescence (F1)
Cycle Number
B
PKC γ
C
IP3R1
D
ITPKC
E
G-Substrate
F
CARP
G
Calbindin
B05
B05xwtUb
B05xK48R

Figure 14. RNA analysis of unchanged genes in the genetic crosses

Quantitative RT-PCR analysis of gene expression in B05, B05 x Wt Ub, and B05 x K48R genetic crosses. No difference in the RNA levels were observed between the mice for A) the AMPA receptor gene, B) the EAAT4 gene, C) the SERCA2 gene, and D) the Homer-3 gene. Graph legends depicting B05 (black), B05 x Wt (blue), and B05 x K48R (red).

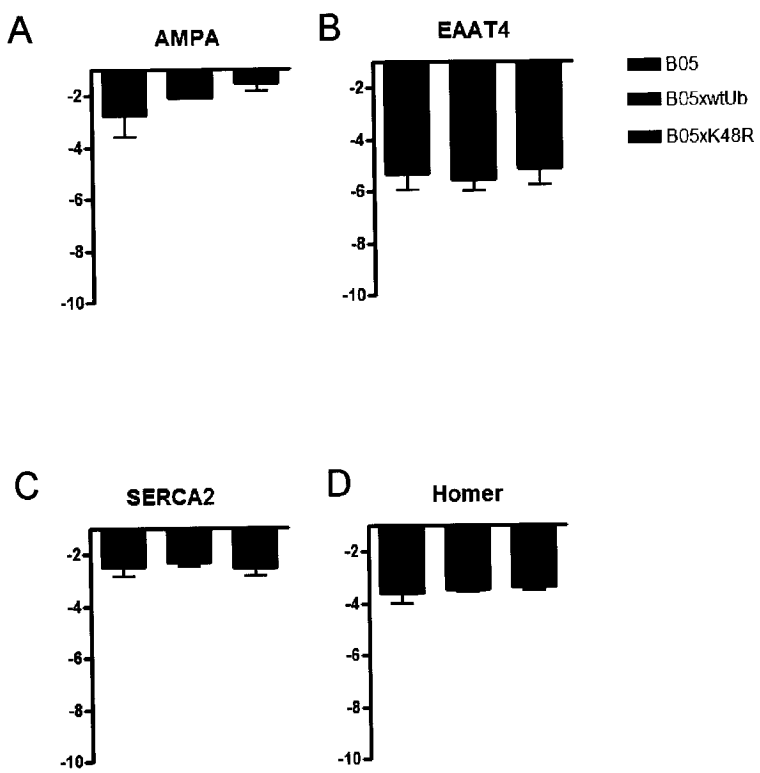
A
AMPA
B
EAAT4
B05
B05xwtUb
B05xK48R
-2
-4
-6
-8
-10
C
SERCA2
D
Homer

downregulated at similar levels to B05 and B05 x wt Ub (Figure 14). Consistent with this finding was the increase levels of phosphorylated polymerase II in genetic crosses (Figure 15).

3.7 Gene-reprogramming by mutant ubiquitin in SCA1 animals is not likely due to an alteration in the number of Purkinje cell neurons

One plausible explanation for the restoration of transcription in the B05 x K48R animals would be the presence of an increased number of Purkinje cell neurons at the time where the animals were sacrificed. To determine if this was the case, the number of Purkinje cells per unit length were counted (Figure 16) on sections that were stained for calbindin. When comparing the Purkinje density between B05, B05 x wtUb, and B05 x K48R mice with the assistance of Zeiss software Axiovision 3.1, there were no significant differences inferring that the loss of gene transcription in B05 animals occurred before a significant reduction of Purkinje cell number and that the restoration of gene transcription in B05 x K48R most likely has occurred at the molecular rather than cellular level.

3.8 No change in Ataxin-1 mRNA levels in compound transgenics at 3-months

The levels of Ataxin-1 have been previously reported to affect the course of SCA1 pathology with higher levels of expression resulting in an earlier and more severe phenotype (Zu et al., 2004). Given the transcriptional differences observed in the genetic crosses, it was possible that the amelioration of the phenotype was a result of reduced expression of ataxin-1. To exclude this possibility, the mRNA levels were determined by Northern blot analysis (Figure 17). No differences were observed in the mRNA levels of transgene derived ataxin-1 in the cerebella of the genetic crosses when compared with

B05 animals.

Figure 15. Analysis of protein levels in the cerebella of 3 month old mice

A) Western blot analysis with a phospho-RNA polymerase specific antibody revealed that the levels were increased in B05 x K48R cross when compared to heterozygous B05 and B05 x Wt Ub mice. B) Western analysis of the same lysates with a PCAF antibody showing no difference in the levels of this histone acetyltransferase. Actin served as a loading control.

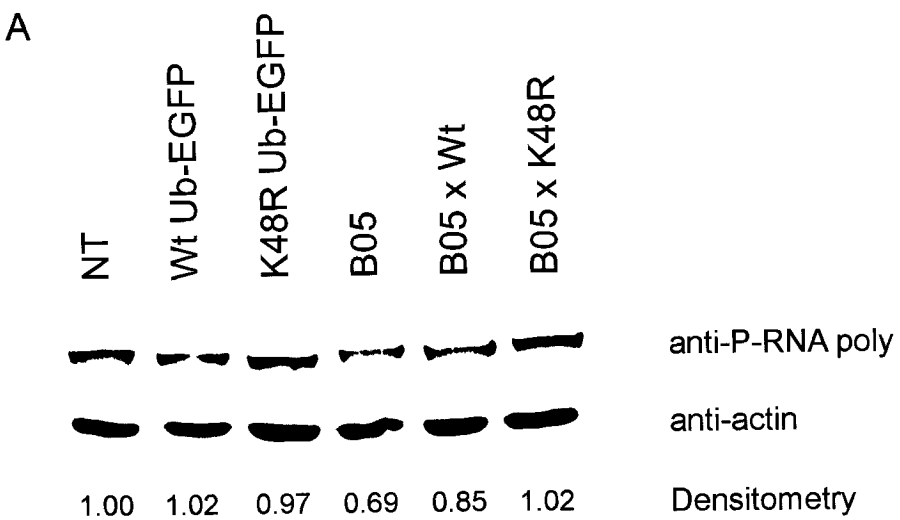
A
NT
Wt Ub-EGFP
K48R Ub-EGFP
B05
B05 x Wt
B05 x K48R
anti-P-RNA poly
anti-actin
1.00
1.02
0.97
0.69
0.85
1.02
Densitometry
B
anti-PCAF
anti-actin

Figure 16. Determination of Purkinje cells density in mouse cerebella

A) Representative images of cerebellar sections that were photographed using the Zeiss software Axiovision 3.1 and used in the determination of the number of Purkinje cells. Purkinje cell density of a given field of view was expressed per unit length. B) Bar graph representing the average number of Purkinje cells per unit length for each genotype. No significant differences were observed between B05 and respective crosses.

A

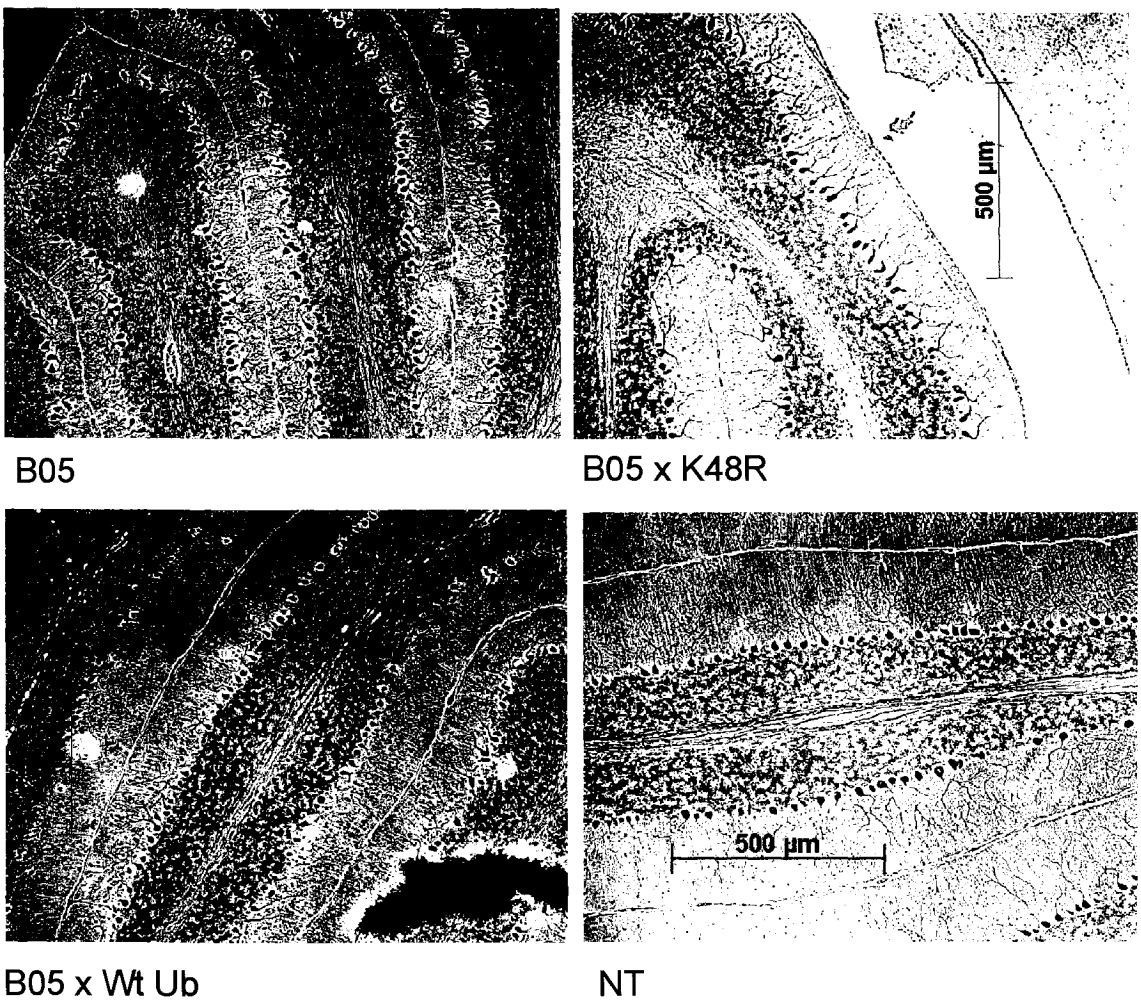

B05

B05 x K48R

B05 x Wt Ub

NT

B

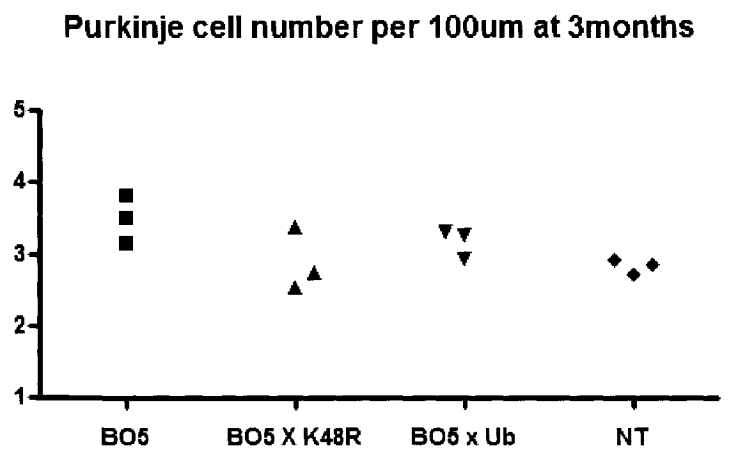

Figure 17. Analysis of the mRNA levels of ataxin-1 in mouse cerebella

Northern blot analysis of total RNA from cerebella of 3 month old straight genotypes and genetic crosses with a cDNA fragment encoding the non-expanded ataxin-1 protein (Q30). The mRNA levels of the transgene-derived expanded ataxin-1 (83Q) did not appear to differ significantly in the cerebella of the genetic crosses when compared with the B05 mice. Endogenous ataxin-1 levels were not detected. A human β-actin cDNA fragment (actin) served as a control for loading.

K48R x B05
Wt Ub x B05
B05
K48R Ub-EGFP
Wt Ub-EGFP
NT
SCA-1
Actin

3.9 Partial restoration of postsynaptic density protein Homer in K48R mice

The stabilization of natural and artificial ubiquitin-proteasome substrates by K48R mutant ubiquitin has been previously reported in cultured mammalian cells (Tsirigotis et al., 2001a) and *in vivo* (Tsirigotis et al., 2001b). It has been previously documented that polyglutamine containing proteins have the ability to sequester transcription factors and alter gene expression of numerous neuronal genes involved in survival pathways (Jiang et al., 2003; Schaffar et al., 2004; Tsuda et al., 2005). It was therefore conceivable, that in the context of SCA1 pathology, K48R mutant ubiquitin may also affect the stability of key molecular proteins involved in synaptic remodelling which would serve in the proper maintenance of synaptic activity. Considering the well documented regulation of postsynaptic density proteins by ubiquitin-mediated proteolysis (Ehlers, 2003), it was speculated that K48R mutant ubiquitin may affect the steady state levels of key modulators otherwise lost throughout the course of SCA1. This hypothesis of restored post density proteins was tested by the analysis of the protein levels of homer and PSD-95 by western blot analysis. The data presented in Figure 18 revealed an increase in the levels of homer whereas no difference in the levels of PSD-95 protein levels were observed.

Figure 18. Western blot analysis of postsynaptic proteins

Western analysis of mouse cerebella at 3 months of age with antibodies raised against A) Homer, and B) PSD-95. Levels of Homer were reduced in the cerebella of B05 heterozygous and B05 x Wt Ub mice but seemed elevated in the B05 x K48R cross. No difference in the protein levels of PCAF were noted in the various strains. C) Actin served as a control for equal loading of protein.

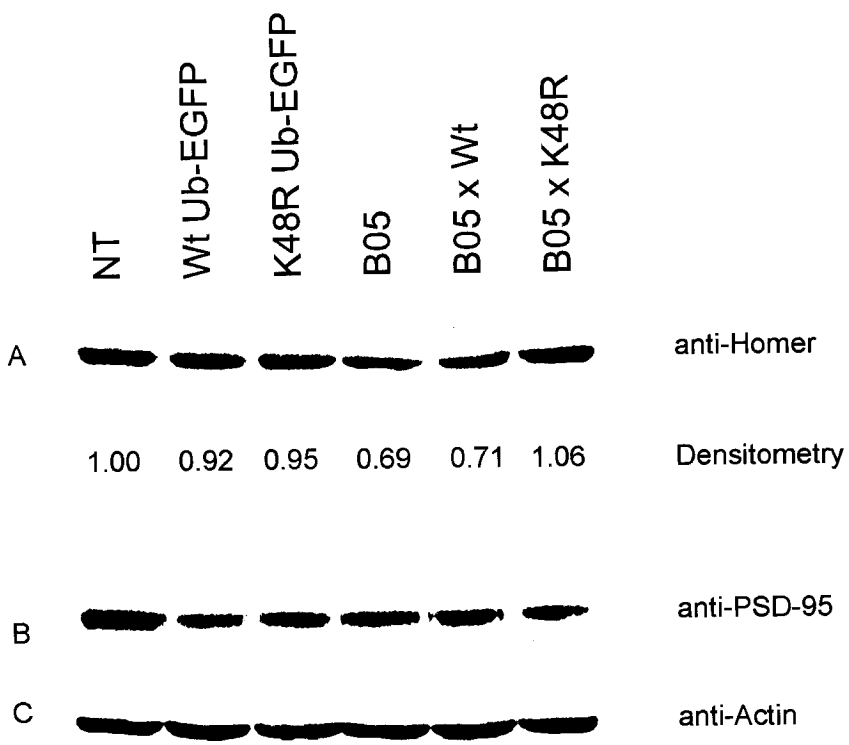
NT
Wt Ub-EGFP
K48R Ub-EGFP
B05
B05 x Wt
B05 x K48R
A
anti-Homer
1.00
0.92
0.95
0.69
0.71
1.06
Densitometry
B
anti-PSD-95
C
anti-Actin

Chapter 4

Discussion

4.1 Generation of novel ubiquitin transgenic mice

The unicellularity of yeast cells combined with the easy manipulation of their genomes has made them the model of choice to study the phenotypes of mutations. In fact, a comprehensive mutational analysis of ubiquitin was originally performed in this model system and has served to elucidate the role of ubiquitin in cellular processes. In recent years, the ability to manipulate the genomes has served as a powerful tool in elucidating the function of genes in the context of a multicellular organism. Consequently, the effects of mutant ubiquitin have been studied in transfected cells of higher eukaryotes (Treier et al., 1994; Ward et al., 1995), and transgenic plants have been generated in which tagged ubiquitin has been used to retrieve ubiquitylated substrates (Ling et al., 2000). Herein, a novel strategy has been adopted to generate ubiquitin transgenic mice expressing either wild type or mutant variants of ubiquitin as linear fusions with EGFP. The objective in creating these transgenic mice was to study the in vivo effects of mutant isoforms of ubiquitin. It has been found that fusions of ubiquitin with EGFP were efficiently recognized and processed in vitro (Tsirigotis et al., 2001a) and *in vivo* (Tsirigotis et al., 2001b)) and that the ubiquitin moieties generated by the co-translational cleavage were incorporated into HMW conjugates (Figure 5). Comparison of endogenous ubiquitin levels in brain lysates of ubiquitin transgenics by western blot analysis with a ubiquitin specific antibody revealed no differences in the levels of total ubiquitin suggesting that the expression of the mutant isoforms does not result in a compensatory induction of endogenous ubiquitin genes (Figure 6). The levels of transgene expression were also not found to differ significantly in the mutant ubiquitin

transgenic lysates as assessed by western analysis with an antibody raised against EGFP suggesting that phenotypic differences would not be accounted by differences in expression. Since their creation, these mice have been utilized to recover *in vivo* substrates of the UPP using standard nickel chromatography approaches (Tsirigotis et al., 2001b), to investigate the role of mutant ubiquitin in response to agents that induce stress (canavanine, paraquat and LPS, aging) and in the study of ubiquitin in normal and diseased conditions (described in a subsequent section).

4.2 Applications of the Real-Time PCR Methodology

The advent Real-Time PCR has allowed scientist to exploit the limitations of conventional PCR and has emerged as a powerful tool in genomics research. Its unique ability to observe in real-time the PCR kinetics using fluorescence DNA binding agents, coupled with the flexibility to adjust PCR parameters (such as denaturing/annealing duration temperature) in a rapid cycling and temperature ramping environment, has made it possible to amplify less abundant DNA templates in a highly efficient and reproducible manner. Real-Time PCR technology has drastically influenced molecular biology research and is now routinely used for nucleic acid diagnostics such viral quantification (Tang-Feldman et al., ; Plumet and Gerlier, 2005), drug therapy efficacy (Erali et al., 2001), DNA damage measurements (Ayala-Torres et al., 2000), pathogen detection (Lindenbach et al., 2005), and allelic discrimination studies (Kees et al., 2005).

While traditional PCR relied on end-point detection by way of gel analysis, Real-Time PCR chemistries allows the user to monitor the entire DNA amplification process in real-time. To demonstrate the advantages of the Real-Time PCR strategy one should consider

a PCR reaction as divided into three phases (exponential, linear, and the plateau or end-point phase). The exponential phase occurs at the beginning of DNA amplification in which the kinetics of the reaction favours the doubling of the product after each cycle. During the linear phase, the reaction efficiency begins to decline as consequence of depletion of the PCR components, eventually resulting in cessation of amplification of the DNA template in the plateau or end-point phase. Since all PCR reactions will inevitably attain the plateau phase, it is difficult to asses whether of the analysis of the final amplification product truly represent the initial amounts of starting material making conventional PCR a non-attractive means of quantification of gene expression. The sensitivity or Real-Time PCR, which utilizes measurements during the exponential phase of the reaction to assess differences in amplicon levels, allows the detection of differences as low as two-fold otherwise overlooked by gel analysis following traditional PCR. By simultaneously combining a standard curve for the target gene and a control curve based on a housekeeping gene coupled to the reduced time in which reactions can be analyzed (1 hour versus 4 hours of user intervention excluding gel analysis and quantification of the products) has rendered RT-PCR the method of choice in the validation/quantification of gene expression (Bustin et al., 2005). In fact, this strategy was used to validate genes identified by microarray analysis in B05 and B05 x ubiquitin crosses.

For the aforementioned reasons, this technology was exploited to establish a genotyping strategy. The rational of this strategy was to maintain ubiquitin transgenic colonies without having to resort to traditional PCR or Southern blotting which would not be informative; both southern blot and traditional PCR analysis would only detect the

presence or absence of the transgene rather than the absence of presence of the mutant transgene. The combinatorial genotyping approach would not be possible with conventional PCR considering that all primers sets would eventually amplify as the reaction kinetics approached the plateau phase. Analysis of the amplification product (from each primer set) by means of gel analysis would not be adequate in differentiation between transgenics strains given that the end-point detection would give rise to bands of equal intensity. Therefore, it was of paramount importance to identify which of the 4 primer combinations initiated the exponential phase and arrested the PCR prior to the reaction reaching the plateau phase.

It was found that this methodology can be used in the accurate genotyping of mice differing by a single point mutation in the transgene DNA. The approach, however, can only be applied for genotyping of mice in which the transgene can be distinguished from the endogenous gene (i.e. the incorporation of an epitope tag, selectable marker of reporter proteins) and in cases where the genomic DNA has not been contaminated by other DNA sequences (see mystery tail test in Table 2). This genotyping strategy has aided in the verification of genotype identification of our colonies, the generation of homozygous strains, and allowed us to generate compound transgenic mice by crossing these mice with the SCA1 mouse model of neurodegeneration (a disease model in which ubiquitin has been implicated).

Given the sensitivity of the methodology, it is possible to use a modified version of the Real-Time PCR strategy to decipher between homozygous versus heterozygous mice by looking at the difference in C_T values. The threshold cycle number (C_T value) is defined

as the cycle number at which fluorescence emission exceeds a fixed threshold above baseline values and is determined during the exponential phase of the PCR reaction. Since there exists a quantitative relationship between the amount of starting material and the amount of PCR product at any given cycle number, the number of cycles requited to reach the threshold value of detection (C_T value) is inversely proportional to the amount of starting DNA. A sample with twice the DNA content would undergo exponential amplification exactly one cycle sooner. Homozygous mice would theoretically carry twice as many copies of the transgene and would therefore amplify once cycle sooner than that of the heterozygous counterpart. By comparing the C_T value of both samples, it would be possible to extrapolate the copy number of the transgene in each strain and hence the genotype. Much like conventional PCR, the Real-Time strategy is sensitive to the concentration of the initial DNA template and it is therefore of prime importance that the amount of DNA utilized in each reaction be equal (a problem that can be easily resolved by assessing the concentration and quality of the DNA with a spectrophotometer). In addition, the efficiency of the primers must be maximal (100%) during the initial exponential phase and easily assessed using the following formula in which E represents efficiency of the PCR reaction (Pfaffl, 2001):

$$E = 10^{-1/slope}$$

A slope of -3.6 to -3.1 is required in order to satisfy the mathematical relationship between the amount of starting material and the amount of PCR product at any given cycle number. PCR efficiency can be measured by constructing a standard curve from a serially diluted standard. If the reaction efficiency is not maximal (100%) the doubling

of the amplicon at every cycle will not correlate with a doubling of transgene product resulting in inaccurate results.

4.3 *In vivo* modulation of SCA1 by K48R mutant ubiquitin

One of the distinguishing features of the conformational diseases is the presence of cytoplasmic and/or nuclear inclusion bodies that co-localize with chaperones and components of the UPP. It is predicted that polyglutamine proteins are recognised by the cell as improperly folded proteins and subjected to either chaperone-mediated refolding or targeting to the proteasome. It is not surprising then that exogenous expression of chaperone proteins can alleviate the phenotype in a variety of cell culture systems and in transgenic mice expressing expanded polyglutamine proteins (Cummings et al., 1998; Cummings et al., 2001; Kobayashi and Sobue, 2001; Adachi et al., 2003). Similarly, it is predicted that interfering with the targeting and degradation of the toxic protein would result in the exacerbation of the phenotype. The data presented here suggest no such deleterious effects but rather a beneficial effect, albeit transient, in the onset and progression of disease; the expression of a chain-terminating variant of ubiquitin (K48R) protected Purkinje neurons from altered migration and ameliorated the performance of ataxic mice as assessed by experiments performed with the rotarod apparatus. This delay in the phenotype is not due to a reduction in Purkinje cell number (Figure 16) or in alterations in the expression of SCA1 (Figure 17) both of which would clarify the amelioration of the disease in the genetic crosses. It also been recently shown not to be accounted by a heat shock response or to alterations in endogenous levels of ubiquitin (Tsirigotis et al., in press). The most plausible explanation for the ability of mutant ubiquitin to delay the pathogenic progression of SCA1 would be that some key cellular

protein or proteins normally subject to ubiquitin-mediated degradation in SCA1 is stabilized by mutant ubiquitin. It has been recently demonstrated that, much like the expanded polyglutamine tracts found within the Huntington and androgen receptor proteins, ataxin-1 has the ability to bind and sequester transcriptional activators ((Tsuda et al., 2005) and reviewed in ((Everett and Wood, 2004))). Amongst proteins that are sequestered by expanded polyglutamine tracts are p300/CBP acetyltransferases (well documented UPP substrates whose degradation has been shown to be enhanced in the presence of expanded polyglutamine containing proteins) which via acetylation of histones influence the transcription of a variety of genes (Tsirigotis et al., in press). Considering the well documented importance of p300/CBP in the maintenance of neuronal homeostasis, it is not unexpected that the loss of function or abundance of these proteins would result in an alteration of gene transcription. Consistent with the postulated homeostatic function of CBP in neural tissues, elimination of CREB in the forebrain using a Cre/lox system has been found to induce neurodegeneration of the hippocampus and striatum, with features reminiscent of Huntington's disease (Mantamadiotis et al., 2002). The sequestration of CBP and therefore the loss of CBP-mediated transcription by Purkinje-specific expression of CREB (a CBP interacting protein) has recently been reported to be the basis for impaired performance of mice on the rotarod apparatus (Brodie et al., 2004). In the context of SCA1, it has been demonstrated that K48R mutant ubiquitin can restore the levels of these acetyltransferesase in the presence of the expanded ataxin-1 protein resulting in an increase in histone H4 acetylation suggesting that this modification is of functional significance with regard to SCA1 (Tsirigotis et al., in press). p300 and CBP are histone acetyltransferases (HAT) whose activities are in opposition to histone deacetylases

HDAC). Reasoning that the loss of HAT activity in polyQ disease could be restored by inhibition of HDACs, several groups have administered pharmacological agents targeting these enzymes in fly (Steffan et al., 2001; Ghosh and Feany, 2004) or mouse transgenic models of polyQ disease (Ferrante et al., 2003; Hockly et al., 2003) and have observed delayed disease progression. Taken together, this data suggested that a beneficial effect can be achieved either through inhibition of HDACs or through stabilization of HATs but did not exclude possible effects of mutant ubiquitin on transcription through mediators other than p300/CBP. It is likely that the ubiquitin/proteasome pathway intersects with transcriptional regulation at many points (Muratani and Tansey, 2003) and is conceivable that the stabilization of other transcriptional factors or co-factors by K48R mutant ubiquitin exerts a potent and beneficial effect on transcription of genes whose loss figures in the course of the disease. In B05 x K48R genetic crosses, it was found that the steady state levels of phosphorylated RNA polymerase II was increased when compared to B05 mice suggesting a more global role of ubiquitin in the regulation of gene transcription (Figure 15). Consistent with a role of ubiquitin in transcription is the recent report demonstrating that the activity of the met4 transcription factor in yeast cells is inhibited by the presence of a K48 linked poly-ubiquitin chain, which acts through a non-proteolytic mechanism (Flick et al., 2004). Although this appears to be an exception rather than a rule, it highlights the complexity of targeting by ubiquitin and suggests that modification of proteins by K48 linked polyubiquitin chains may serve transient, non-proteolytic roles. It is presently unknown whether transcription factors in higher eukaryotes are subject to similar regulation, but if this were the case it is conceivable to imagine how the expression of K48R mutant ubiquitin might serve a role in reprogramming gene expression by modulating the activity of key transcriptional

regulators. There is accumulating evidence suggesting transient ubiquitin-mediated activation of transcription factors may precede their proteolytic degradation (Muratani and Tansey, 2003). Although the order of events in SCA1 is still not entirely clear, there is ample evidence that perturbation of transcription plays an early and important role. Through a subtractive cloning approach Lin *et al.* identified genes whose downregulation occurred before overt pathology in the B05 mouse model and in SCA1 patient tissues (Cummings and Zoghbi, 2000; Lin et al., 2000). By the time pathology is apparent, microarray analysis demonstrates a substantially altered pattern of gene expression in B05 cerebella as compared to age-matched controls (Figure 11). The genes that were found to be altered pointed to a dysregulation in calcium and glutamate homeostasis which have been speculated to contribute to disease progression (Table 3 and see section 4.4).

4.4 Interplay between calcium and glutamate signalling in SCA1

The common mechanism of neuronal injury and death in many neurodegenerative diseases is the destructive metabolic pathway involving the excessive activation of neuronal amino acid receptors(Lerma et al., 1993; Mark et al., 2001; Tateno et al., 2004). The emerging role of glutamate in neuronal diseases is currently under intense investigation in the hope of elucidating the molecular mechanism underlining neuronal death induced by glutamate excitotoxicity (excessive activation of neuronal amino acid receptors). Glutamate is an abundant neuronal amino acid neurotransmitter and signalling molecule that is released by exocytosis in the synaptic space in a highly regulated manner (Mark et al., 2001). In normal synaptic functioning, activation of excitatory amino acid receptors is transitory and it is therefore not unexpected that

prolonged or excessive glutamate signalling may result in altered neuronal homeostasis. Consistent with this is the well documented cellular death that occurs in neuronal cultures when exposed to an excess of glutamate. This process of neuronal death is referred to excitotoxicity and appears to involve a multifactorial process including ROS formation, mitochondrial dysfunction and sustained elevations of intracellular calcium levels (Cho et al., 2001; Arundine and Tymianski, 2003; Brustovetsky et al., 2005). Binding of glutamate to its cognate receptors has been shown to a play an important role in synaptic plasticity including long-term potentiation (LTP) and long-term depression (LTD), processes that underlie learning and memory (Lisman, 2001; Lisman et al., 2003). The signalling cascade triggered by glutamate activation in non-pathogenic synapses in schematically depicted in Figure 19. In response to a synaptic signal, glutamate is released by exocytosis at the presynaptic clef and binds to metabotropic glutamate receptors (mGluR) at the plasma membrane of the Purkinje cell. This interaction results in the triggering of a G-couple proteins signalling cascade involving phospholipase C (PLC) which initiates the production of inositol-1,4,5-triphosphate (IP3) and diacyl-glycerol (DAG). Whereas IP3 diffuses and binds to its receptor (IP3R1) on the ER resulting in a local release of calcium from intracellular calcium stores in small dendritic regions, DAG serves in the activation of signalling cascades resulting in the activation of PKC. The interaction between IP3R1 and mGluR is facilitated by molecular scaffold proteins such as homer which bring these two receptors in close proximity. The binding of IP3 to IP3R1 is antagonized by a molecule termed CARP whose function is to bind the receptor and decrease its affinity for IP3. The calcium buffering protein calbindin and the calcium ATPase pump SERCA work synergistically to counter-act excessive calcium release. In B05 mice, it was found that the expression of these genes was greatly reduced

Figure 19. A schematic model of the glutamate signalling pathway at the postsynaptic membrane of Purkinje cells

Activation of mGluR results in the production of IP3 through G-coupled proteins and PLC. IP3 diffuses into the cytoplasm and binds to IP3R located on the ER membrane causing the release of intracellular stores of Ca^{2+}. Glutamate signalling also results in the activation of the AMPA receptor resulting in the depolarization of the membrane potential and the activation of VGCC which leads to an influx of Ca^{2+} in the cytoplasm. Homer serves as an adaptor protein to link mGluR signalling to IP3R1. CARP is an intracellular molecule that binds to IP3R thus reducing the affinity of the receptor to IP3. This interaction can modulate the amount of calcium to be released. High intracellular Ca^{2+} levels activate PKC leading to the internalization of the AMPA receptor. This interaction is counter-acted by PP2A. G-substrate can enhance the internalization of the AMPA receptor by inhibiting PP2A. PSD-95 serves as a molecular scaffold that interacts with glutamate receptors. Excess glutamate is removed by EAAT4 preventing excitotoxicity. Ca^{2+} is removed by SERCA2 or buffered by the buffering protein calbindin. Abbreviations: G, Glutamine; mGluR, metabotrobic glutamate receptor; AMPARmemb, Alpha-amino-3-hydroxy-5-methylisoxazole-4-propionic acid Receptor at the membrane; AMPARinternal, Alpha-amino-3-hydroxy-5-methylisoxazole-4-propionic acid Receptor internalized; EAAT4, glutamate excitatory amino acid transporter type 4; VGCC, Voltage gated calcium channel; PLC, phospholipase C; IP3, inositol 1,4,5-triphosphate; IP3R, inositol 1,4,5-triphosphate receptor; ER, endoplasmic reticulum; CARP, carbonic anhydrase-related protein; SERCA2, Sarcoendoplasmic reticulum Ca^{2+}-ATPase type 2; PP2A, protein phosphatase 2A; PKC, Protein kinase C; PSD-95, postsynaptic density-95.

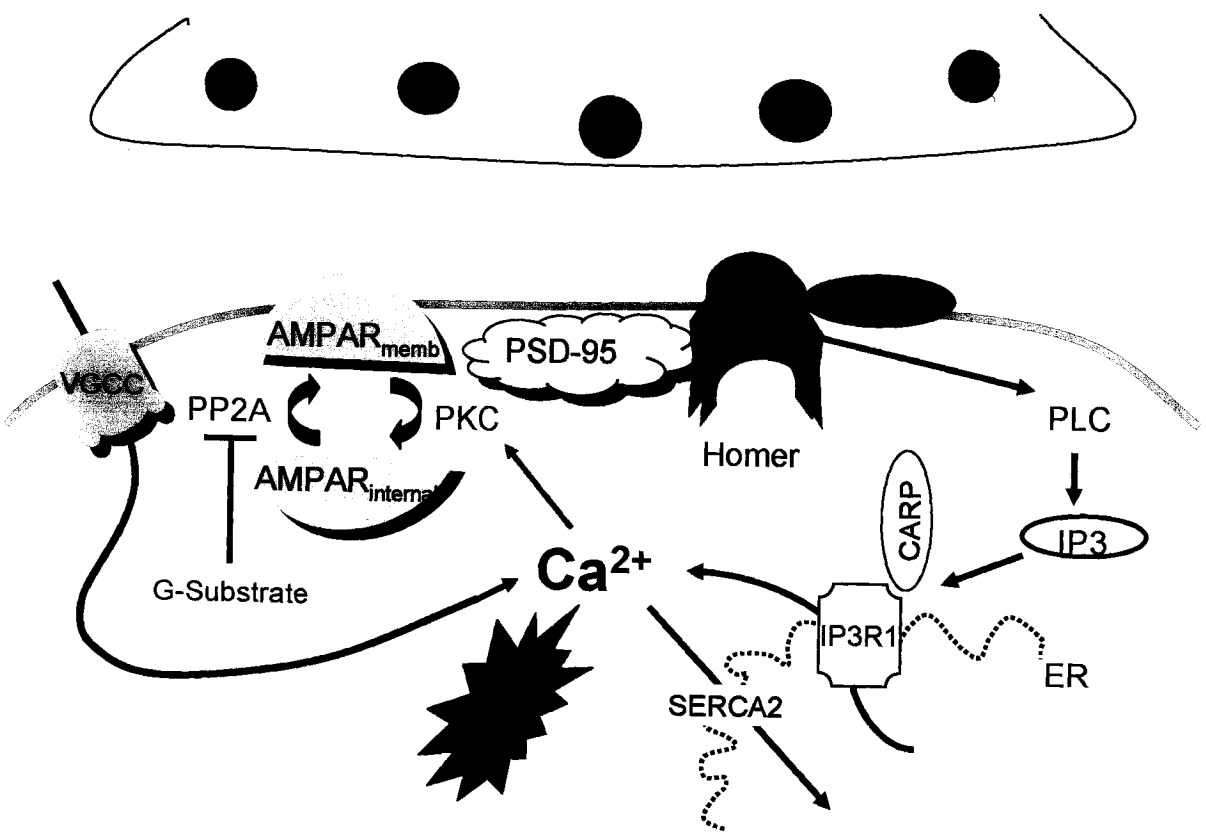
AMPAR$_{memb}$
PSD-95
VGCC
PP2A
PKC
Homer
PLC
AMPAR$_{internal}$
CARP
IP3
G-Substrate
Ca^{2+}
IP3R1
ER
SERCA2

suggesting that in the course of SCA1 a high level of calcium may be the basis for impaired motor coordination and learning. It is conceivable that the downregulation of genes involved in calcium release in SCA1 mice reflects a compensatory mechanism to decrease the levels of intracellular calcium. There is accumulating evidence that calcium can trigger biochemical events that can either weaken or strengthen synapses and in essence, calcium acts as a second messenger in both long-term potentiation (LTP) and long-term depression (LTD). It has been recently suggested that the level of calcium determines whether LTP or LTD occurs with higher levels of calcium triggering LTP and lower levels triggering LTD (Lisman and Spruston, 2005). Consistent with the role of calcium in modulating these processes are the behavioural consequences and motor neuron deficiencies readily observed in Huntington's (Tang et al., 2003; Tang et al., 2005), ALS (Tateno et al., 2004), Alzheimer's (Stutzmann et al., 2004; Braunewell, 2005), and other neurodegenerative diseases (Zhuchenko et al., 1997; Cho et al., 2001; Arundine and Tymianski, 2003). This supposition is also supported by the well documented requirement of IP3R in the maintainance of LTD (Inoue et al., 1998; Nagase et al., 2003) and the finding that IP3R knockout mice (which display little alterations in Purkinje cell structure, excitability or synaptic connections) are completely deficient in the ability to induce LTD (Matsumoto et al., 1996). Taken together, these data suggest that SCA1 mice are deficient in triggering a productive LTD and indirectly suggest that they may be suffering from excitotoxicity due to excess glutamate. This is supported by the finding that EAAT4, whose primary function is to remove excess glutamate (Huang et al., 2004), is significantly downregulated in B05 mice. In addition to the activation of mGluR, glutamate has been shown to activate the AMPA receptor(Perez-Otano and Ehlers, 2005). Activation of the latter results in the depolarization of the membrane and a

in a large influx of extra cellular calcium via the voltage gated calcium channels (VGCC). Similarly to mGluR, the stimulation of the AMPA receptor by glutamate results its internalization from the Purkinje cell membrane. The recycling of the AMPA receptor is a tightly regulated process involving numerous signalling molecules. Amongst these regulators are protein kinase C (PKC) and protein phosphatase 2A (PP2A); whereas PKC phosphorylates the receptor resulting in its internalization, PP2A opposes the action of PKC to maintain it at the membrane. Both of these processes are also subject to regulation by either scaffolding proteins such as postsynaptic density protein 95 (PSD-95) who assist in the recycling of the AMPA receptor to the plasma membrane or by G-substrate that antagonizes PP2A (thereby helping in the internalization the receptor). The observation of reduced expression G-substrate in B05 mice suggests a dysregulation in PP2A activity which would favour the maintenance of the AMPA receptor at the plasma membrane. Since proper LTD requires a balance in the internalization/recycling of the AMPA receptor, it is plausible that SCA1 have a deficiency in LTD. This is consistent with a recent report showing that a trinucleotide expansion in the gene encoding the regulatory subunit of PP2A results in SCA12 with features recapitulating the pathogenesis of SCA1 (Holmes et al., 2001). The downregulation of G-substrate in SCA1 mice may reflect a compensatory mechanism to maintain the receptor at the cell surface suggesting that Purkinje neurons may be suffering from excess glutamate mediated endocytosis of the AMPA receptor.

The data suggest that the restoration of these genes in the B05 x K48R mice may be of functional significance to SCA1. The finding of an improvement in gene transcription of important synaptic modulators coupled with the enhanced stability of a least one protein

involved in the reorganisation of the synapse (homer) suggest that the expression of K48R mutant ubiquitin may play a role in the restoration of LTD. Considering the well documented importance of LTD in processes such as neuronal plasticity, learning and memory it is conceivable that these molecular changes are the basis for improved rotarod performance and delay in the deterioration of Purkinje cell morphology in the genetic crosses.

Based on previous results, it is clear that the stabilization of transcription factors or co-factors by K48R mutant ubiquitin has beneficial consequences on the transcription of neuronal genes otherwise lost in SCA-1. The data presented herein suggest that it is also likely that K48R mutant ubiquitin acts in the stabilization of synaptic proteins as evidenced by the increase in the homer protein in the genetic cross (Figure 18) and to a more global reprogramming of gene transcription (Figure 13). It is possible that the modulation of gene transcription by K48R mutant ubiquitin of genes whose protein products are not subject to ubiquitin-mediated turnover following synaptic activity benefits long-term structural and functional changes at the synapse. However, considering the lengthy time required for *de novo* transcription of genes and protein synthesis to occur during synaptic remodelling, as opposed to immediate effects of their removal by the UPP as a consequence of synaptic signalling, it is more likely that the synergistic effects of increased transcription of genes coupled with the stabilization of key synaptic modulators by K48R ubiquitin may contribute in safeguarding Purkinje cell neurons in peril. Further experiments may be required to assess this. Given the complexity of interactions occurring at the synapse and the difficulty involved in manipulating these systems *in vivo,* it was reasoned that the molecular interactions may

be best deciphered in primary cerebellar cultures. The benefits of using an *in vitro* system would include the effortless administration of pharmacological agents (such as AMPA, mGluR agonist/antagonist) that stimulate synaptic remodelling or the use of RNAi methodologies to selectively eliminate genes of interest to assist in distinguishing between increase neuronal transcription and synaptic protein abundance. Whether it be comparing levels of synaptic proteins by western blot analysis or measuring the amounts of glutamate and/or calcium subsequent to exposure to various agents, these cultures would prove of great utility in the understanding of SCA-1 and of the modulating role of ubiquitin. These cultures have recently been successfully initiated (Figure 20) and the proposed experiments are currently underway.

Left unresolved are the transient nature of the ameliorated phenotype in the B05 x K48R cross and the partial restoration of genes in the B05 x Wt Ub cross. The basis for the latter is currently unclear but may potentially be explained by a threshold effect that must be reached at the cellular and organismal level that has not been reached. Further experiments are required to determine this.

4.5 Conclusion

In this thesis, the role of ubiquitin in the progression of SCA-1 was examined by generating compound transgenic mice. The data suggest that the expression of a chain-terminating variant of ubiquitin delayed the progression of the disease as assessed by morphological and behaviour measures via mechanism involving gene reprogramming and by enhancing the stability of key substrates involved in synaptic remodelling. It is currently unclear whether the delay in the phenotype is attributed to an amelioration of

Figure 20. Expression of GFAP and calbindin in primary cerebellar cultures

Immunofluorescence staining of cerebellar primary cultures derived from transgenic mice with A) calbindin-specific antibody (red) or B) antibody specific for calbindin (red) and GFAP (green) respectively. Nuclei were counterstained with DAPI. Cells labeled with calbindin represent Purkinje neurons whereas GFAP labeled glia cells. The extensive dendritic growth is indicative of the differentiated state of the Purkinje neurons. Images were taken using a 40X objective.

A

B

LTD (this model obviously awaits validation of protein levels by western blot analysis) or through enhanced stability of yet unidentified transcriptional activators. The primary cultures established should prove of great utility in deciphering the cellular mechanism underlying pathology and the protective effects exerted by expression K48R mutant ubiquitin.

Small molecule inhibitors of the proteasome show promise in clinical trials for oncological disorders such as multiple myeloma (Adams, 2004), proteasomal inhibition has been shown to delay Wallerian degeneration *in vivo* (Zhai et al., 2003) and more recently to suppress polyglutamine-induced nuclear inclusions in cultured post-mitotic neurons (Kim et al., 2004). The data presented herein suggest that the combinatorial effect of prolonging the life of key proteins or by modulating gene expression, K48R mutant ubiquitin may prove beneficial in the context of neurodegenerative diseases.

References

Adachi H, Katsuno M, Minamiyama M, Sang C, Pagoulatos G, Angelidis C, Kusakabe M, Yoshiki A, Kobayashi Y, Doyu M, Sobue G (2003) Heat Shock Protein 70 Chaperone Overexpression Ameliorates Phenotypes of the Spinal and Bulbar Muscular Atrophy Transgenic Mouse Model by Reducing Nuclear-Localized Mutant Androgen Receptor Protein. J Neurosci 23:2203-2211.

Adams J (2004) THE PROTEASOME: A SUITABLE ANTINEOPLASTIC TARGET. Nature Reviews Cancer
Nat Rev Cancer 4:349-360.

Arnason T, Ellison MJ (1994) Stress resistance in Saccharomyces cerevisiae is strongly correlated with assembly of a novel type of multiubiquitin chain. Mol Cell Biol 14:7876-7883.

Arrasate M, Mitra S, Schweitzer ES, Segal MR, Finkbeiner S (2004) Inclusion body formation reduces levels of mutant huntingtin and the risk of neuronal death. 431:805-810.

Arundine M, Tymianski M (2003) Molecular mechanisms of calcium-dependent neurodegeneration in excitotoxicity. Cell Calcium 34:325-337.

Ayala-Torres S, Chen Y, Svoboda T, Rosenblatt J, Van Houten B (2000) Analysis of Gene-Specific DNA Damage and Repair Using Quantitative Polymerase Chain Reaction. Methods 22:135-147.

Baker RT, Board PG (1991) The human ubiquitin-52 amino acid fusion protein gene shares several structural features with mammalian ribosomal protein genes. Nucleic Acids Res 19:1035-1040.

Bence NF, Sampat RM, Kopito RR (2001) Impairment of the ubiquitin-proteasome system by protein aggregation. Science 292:1552-1555.

Braun BC, Glickman M, Kraft R, Dahlmann B, Kloetzel PM, Finley D, Schmidt M (1999) The base of the proteasome regulatory particle exhibits chaperone-like activity. Nat Cell Biol 1:221-226.

Braunewell K-H (2005) The darker side of Ca2+ signaling by neuronal Ca2+-sensor proteins: from Alzheimer's disease to cancer. Trends in Pharmacological Sciences 26:345-351.

Brodie CR, Khaliq M, Yin JCP, Brent Clark H, Orr HT, Boland LM (2004) Overexpression of CREB reduces CRE-mediated transcription: behavioral and cellular analyses in transgenic mice. Molecular and Cellular Neuroscience 25:602-611.

Brower CS, Sato S, Tomomori-Sato C, Kamura T, Pause A, Stearman R, Klausner RD, Malik S, Lane WS, Sorokina I, Roeder RG, Conaway JW, Conaway RC (2002) Mammalian mediator subunit mMED8 is an Elongin BC-interacting protein that can assemble with Cul2 and Rbx1 to reconstitute a ubiquitin ligase. Proc Natl Acad Sci U S A 99:10353-10358.

Brustovetsky N, LaFrance R, Purl KJ, Brustovetsky T, Keene CD, Low WC, Dubinsky JM (2005) Age-Dependent Changes in the Calcium Sensitivity of Striatal Mitochondria in Mouse Models of Huntington's Disease. Journal of Neurochemistry 93:1361-1370.

Bustin SA, Benes V, Nolan T, Pfaffl MW (2005) Quantitative real-time RT-PCR - a perspective. J Mol Endocrinol 34:597-601.

Chen H-K, Fernandez-Funez P, Acevedo SF, Lam YC, Kaytor MD, Fernandez MH, Aitken A, Skoulakis EMC, Orr HT, Botas J, Zoghbi HY (2003) Interaction of Akt-Phosphorylated Ataxin-1 with 14-3-3 Mediates Neurodegeneration in Spinocerebellar Ataxia Type 1. Cell 113:457-468.

Cho K, Aggleton JP, Brown MW, Bashir ZI (2001) An experimental test of the role of postsynaptic calcium levels in determining synaptic strength using perirhinal cortex of rat. J Physiol (Lond) 532:459-466.

Cummings CJ, Zoghbi HY (2000) Fourteen and counting: unraveling trinucleotide repeat diseases. Hum Mol Genet 9:909-916.

Cummings CJ, Mancini MA, Antalffy B, DeFranco DB, Orr HT, Zoghbi HY (1998) Chaperone suppression of aggregation and altered subcellular proteasome localization imply protein misfolding in SCA1. Nat Genet 19:148-154.

Cummings CJ, Sun Y, Opal P, Antalffy B, Mestril R, Orr HT, Dillmann WH, Zoghbi HY (2001) Over-expression of inducible HSP70 chaperone suppresses neuropathology and improves motor function in SCA1 mice. Hum Mol Genet 10:1511-1518.

Cummings CJ, Reinstein E, Sun Y, Antalffy B, Jiang Y, Ciechanover A, Orr HT, Beaudet AL, Zoghbi HY (1999) Mutation of the E6-AP ubiquitin ligase reduces nuclear inclusion frequency while accelerating polyglutamine-induced pathology in SCA1 mice. Neuron 24:879-892.

Deng L, Wang C, Spencer E, Yang L, Braun A, You J, Slaughter C, Pickart C, Chen ZJ (2000) Activation of the IkappaB kinase complex by TRAF6 requires a dimeric ubiquitin-conjugating enzyme complex and a unique polyubiquitin chain. Cell 103:351-361.

Ehlers MD (2003) Activity level controls postsynaptic composition and signaling via the ubiquitin-proteasome system. 6:231-242.

Erali M, Page S, Reimer LG, Hillyard DR (2001) Human Immunodeficiency Virus Type 1 Drug Resistance Testing: a Comparison of Three Sequence-Based Methods. J Clin Microbiol 39:2157-2165.

Everett CM, Wood NW (2004) Trinucleotide repeats and neurodegenerative disease. Brain 127:2385-2405.

Ferrante RJ, Kubilus JK, Lee J, Ryu H, Beesen A, Zucker B, Smith K, Kowall NW, Ratan RR, Luthi-Carter R, Hersch SM (2003) Histone deacetylase inhibition by sodium butyrate chemotherapy ameliorates the neurodegenerative phenotype in Huntington's disease mice. J Neurosci 23:9418-9427.

Flick K, Ouni I, Wohlschlegel JA, Capati C, McDonald WH, Yates JR, Kaiser P (2004) Proteolysis-independent regulation of the transcription factor Met4 by a single Lys 48-linked ubiquitin chain. Nat Cell Biol 6:634-641.

Ghosh S, Feany MB (2004) Comparison of pathways controlling toxicity in the eye and brain in Drosophila models of human neurodegenerative diseases. Hum Mol Genet 13:2011-2018.

Glickman MH, Ciechanover A (2002) The Ubiquitin-Proteasome Proteolytic Pathway: Destruction for the Sake of Construction. Physiol Rev 82:373-428.

Glickman MH, Rubin DM, Coux O, Wefes I, Pfeifer G, Cjeka Z, Baumeister W, Fried VA, Finley D (1998) A subcomplex of the proteasome regulatory particle required for ubiquitin-conjugate degradation and related to the COP9-signalosome and eIF3. Cell 94:615-623.

Gray DA, Tsirigotis M, Woulfe J (2003) Ubiquitin, proteasomes, and the aging brain. Sci Aging Knowledge Environ 2003:RE6.

Haglund K, Shimokawa N, Szymkiewicz I, Dikic I (2002) Cbl-directed monoubiquitination of CIN85 is involved in regulation of ligand-induced degradation of EGF receptors. PNAS 99:12191-12196.

Hilt W, Wolf DH (1995) Proteasomes of the yeast S. cerevisiae: genes, structure and functions. Mol Biol Rep 21:3-10.

Hockly E, Richon VM, Woodman B, Smith DL, Zhou X, Rosa E, Sathasivam K, Ghazi-Noori S, Mahal A, Lowden PA, Steffan JS, Marsh JL, Thompson LM, Lewis CM, Marks PA, Bates GP (2003) Suberoylanilide hydroxamic acid, a histone deacetylase inhibitor, ameliorates motor deficits in a mouse model of Huntington's disease. Proc Natl Acad Sci U S A 100:2041-2046.

Holmes SE, Hearn EOr, Ross CA, Margolis RL (2001) SCA12: an unusual mutation leads to an unusual spinocerebellar ataxia. Brain Research Bulletin 56:397-403.

Huang YH, Dykes-Hoberg M, Tanaka K, Rothstein JD, Bergles DE (2004) Climbing Fiber Activation of EAAT4 Transporters and Kainate Receptors in Cerebellar Purkinje Cells. J Neurosci 24:103-111.

Inoue T, Kato K, Kohda K, Mikoshiba K (1998) Type 1 Inositol 1,4,5-Trisphosphate Receptor Is Required for Induction of Long-Term Depression in Cerebellar Purkinje Neurons. J Neurosci 18:5366-5373.

Irwin S, Vandelft M, Pinchev D, Howell JL, Graczyk J, Orr HT, Truant R (2005) RNA association and nucleocytoplasmic shuttling by ataxin-1. J Cell Sci 118:233-242.

Jiang H, Nucifora FC, Jr., Ross CA, DeFranco DB (2003) Cell death triggered by polyglutamine-expanded huntingtin in a neuronal cell line is associated with degradation of CREB-binding protein. Hum Mol Genet 12:1-12.

Kao C-F, Hillyer C, Tsukuda T, Henry K, Berger S, Osley MA (2004) Rad6 plays a role in transcriptional activation through ubiquitylation of histone H2B. Genes Dev 18:184-195.

Katzmann DJ, Babst M, Emr SD (2001) Ubiquitin-Dependent Sorting into the Multivesicular Body Pathway Requires the Function of a Conserved Endosomal Protein Sorting Complex, ESCRT-I. Cell 106:145-155.

Kees UR, Terry PA, Ford J, Everett J, Murch A, Klerk Nd, Baker DL (2005) Detection of hemizygous deletions in genomic DNA from leukaemia specimens for the diagnosis of patients. Leukemia Research 29:165-171.

Kim WY, Horbinski C, Sigurdson W, Higgins D (2004) Proteasome inhibitors suppress formation of polyglutamine-induced nuclear inclusions in cultured postmitotic neurons. J Neurochem 91:1044-1056.

Kobayashi Y, Sobue G (2001) Protective effect of chaperones on polyglutamine diseases. Brain Research Bulletin 56:165-168.

Lerma J, Paternain A, Naranjo J, Mellstrom B (1993) Functional Kainate-Selective Glutamate Receptors in Cultured Hippocampal Neurons. PNAS 90:11688-11692.

Lin X, Antalffy B, Kang D, Orr HT, Zoghbi HY (2000) Polyglutamine expansion down-regulates specific neuronal genes before pathologic changes in SCA1. Nat Neurosci 3:157-163.

Lindenbach BD, Evans MJ, Syder AJ, Wolk B, Tellinghuisen TL, Liu CC, Maruyama T, Hynes RO, Burton DR, McKeating JA, Rice CM (2005) Complete Replication of Hepatitis C Virus in Cell Culture. Science 309:623-626.

Ling R, Colon E, Dahmus ME, Callis J (2000) Histidine-tagged ubiquitin substitutes for wild-type ubiquitin in Saccharomyces cerevisiae and facilitates isolation and identification of in vivo substrates of the ubiquitin pathway. Anal Biochem 282:54-64.

Lisman J, Spruston N (2005) Postsynaptic depolarization requirements for LTP and LTD: a critique of spike timing-dependent plasticity. 8:839-841.

Lisman J, Lichtman JW, Sanes JR (2003) LTP: PERILS AND PROGRESS. Nature Reviews Neuroscience
Nat Rev Neurosci 4:926-929.

Lisman JE (2001) Three Ca2+ levels affect plasticity differently: the LTP zone, the LTD zone and no man's land. J Physiol (Lond) 532:285-.

Mantamadiotis T, Lemberger T, Bleckmann SC, Kern H, Kretz O, Martin Villalba A, Tronche F, Kellendonk C, Gau D, Kapfhammer J, Otto C, Schmid W, Schutz G (2002) Disruption of CREB function in brain leads to neurodegeneration. Nat Genet 31:47-54.

Mark LP, Prost RW, Ulmer JL, Smith MM, Daniels DL, Strottmann JM, Brown WD, Hacein-Bey L (2001) Pictorial Review of Glutamate Excitotoxicity: Fundamental Concepts for Neuroimaging. AJNR Am J Neuroradiol 22:1813-1824.

Matsumoto M, Nakagawa T, Inoue T, Nagata E, Tanaka K, Takano H, Kuno J, Sakakibara S, Yamada M, Yoneshima H, Miyawaki A, Furuichi Y, Okano H, Mikoshiba SK, Noda T (1996) Ataxia and epileptic seizures in mice lacking type 1 inositol 1,4,5-trisphosphate receptor. 379:168-171.

Muratani M, Tansey WP (2003) How the ubiquitin-proteasome system controls transcription. Nat Rev Mol Cell Biol 4:192-201.

Nagase T, Ito K-I, Kato K, Kaneko K, Kohda K, Matsumoto M, Hoshino A, Inoue T, Fujii S, Kato H, Mikoshiba K (2003) Long-term potentiation and long-term depression in hippocampal CA1 neurons of mice lacking the IP3 type 1 receptor. Neuroscience 117:821-830.

Orlowski M, Cardozo C, Michaud C (1993) Evidence for the presence of five distinct proteolytic components in the pituitary multicatalytic proteinase complex. Properties of two components cleaving bonds on the carboxyl side of branched chain and small neutral amino acids. Biochemistry 32:1563-1572.

Orr HT (2000) The Ins and Outs of a Polyglutamine Neurodegenerative Disease: Spinocerebellar Ataxia Type 1 (SCA1). Neurobiology of Disease 7:129-134.

Patnaik A, Chau V, Wills JW (2000) Ubiquitin is part of the retrovirus budding machinery. Proc Natl Acad Sci U S A 97:13069-13074.

Perez-Otano I, Ehlers MD (2005) Homeostatic plasticity and NMDA receptor trafficking. Trends in Neurosciences 28:229-238.

Pfaffl MW (2001) A new mathematical model for relative quantification in real-time RT-PCR. Nucl Acids Res 29:e45-.

Pickart CM, Cohen RE (2004) Proteasomes and their kin: proteases in the machine age. Nat Rev Mol Cell Biol 5:177-187.

Plafker SM, Plafker KS, Weissman AM, Macara IG (2004) Ubiquitin charging of human class III ubiquitin-conjugating enzymes triggers their nuclear import. J Cell Biol 167:649-659.

Plumet S, Gerlier D (2005) Optimized SYBR green real-time PCR assay to quantify the absolute copy number of measles virus RNAs using gene specific primers. Journal of Virological Methods 128:79-87.

Redman KL, Rechsteiner M (1988) Extended reading frame of a ubiquitin gene encodes a stable, conserved, basic protein. J Biol Chem 263:4926-4931.

Schaffar G, Breuer P, Boteva R, Behrends C, Tzvetkov N, Strippel N, Sakahira H, Siegers K, Hayer-Hartl M, Hartl FU (2004) Cellular Toxicity of Polyglutamine Expansion Proteins: Mechanism of Transcription Factor Deactivation. Molecular Cell 15:95-105.

Serra HG, Byam CE, Lande JD, Tousey SK, Zoghbi HY, Orr HT (2004) Gene profiling links SCA1 pathophysiology to glutamate signaling in Purkinje cells of transgenic mice. Hum Mol Genet 13:2535-2543.

Shringarpure R, Grune T, Mehlhase J, Davies KJ (2003) Ubiquitin conjugation is not required for the degradation of oxidized proteins by proteasome. J Biol Chem 278:311-318.

Spence J, Sadis S, Haas AL, Finley D (1995) A ubiquitin mutant with specific defects in DNA repair and multiubiquitination. Mol Cell Biol 15:1265-1273.

Steffan JS, Bodai L, Pallos J, Poelman M, McCampbell A, Apostol BL, Kazantsev A, Schmidt E, Zhu YZ, Greenwald M, Kurokawa R, Housman DE, Jackson GR, Marsh JL, Thompson LM (2001) Histone deacetylase inhibitors arrest polyglutamine-dependent neurodegeneration in Drosophila. Nature 413:739-743.

Stutzmann GE, Caccamo A, LaFerla FM, Parker I (2004) Dysregulated IP3 Signaling in Cortical Neurons of Knock-In Mice Expressing an Alzheimer's-Linked Mutation in Presenilin1 Results in Exaggerated Ca2+ Signals and Altered Membrane Excitability. J Neurosci 24:508-513.

Sun Z-W, Allis CD (2002) Ubiquitination of histone H2B regulates H3 methylation and gene silencing in yeast. Nature 418:104-108.

Tang T-S, Tu H, Chan EYW, Maximov A, Wang Z, Wellington CL, Hayden MR, Bezprozvanny I (2003) Huntingtin and Huntingtin-Associated Protein 1 Influence Neuronal Calcium Signaling Mediated by Inositol-(1,4,5) Triphosphate Receptor Type 1. Neuron 39:227-239.

Tang T-S, Slow E, Lupu V, Stavrovskaya IG, Sugimori M, Llinas R, Kristal BS, Hayden MR, Bezprozvanny I (2005) Disturbed Ca2+ signaling and apoptosis of medium spiny neurons in Huntington's disease. PNAS 102:2602-2607.

Tang-Feldman YJ, Wojtowicz A, Lochhead GR, Hale MA, Li Y, Pomeroy C Use of quantitative real-time PCR (qRT-PCR) to measure cytokine transcription and viral load in murine cytomegalovirus infection. Journal of Virological Methods In Press, Corrected Proof.

Tateno M, Sadakata H, Tanaka M, Itohara S, Shin R-M, Miura M, Masuda M, Aosaki T, Urushitani M, Misawa H, Takahashi R (2004) Calcium-permeable AMPA receptors promote misfolding of mutant SOD1 protein and development of amyotrophic lateral sclerosis in a transgenic mouse model. Hum Mol Genet 13:2183-2196.

Treier M, Staszewski LM, Bohmann D (1994) Ubiquitin-dependent c-Jun degradation in vivo is mediated by the delta domain. Cell 78:787-798.

Tsirigotis M, Zhang M, Chiu RK, Wouters BG, Gray DA (2001a) Sensitivity of Mammalian Cells Expressing Mutant Ubiquitin to Protein-damaging Agents. J Biol Chem 276:46073-46078.

Tsirigotis M, Thurig S, Dube M, Vanderhyden BC, Zhang M, Gray DA (2001b) Analysis of ubiquitination in vivo using a transgenic mouse model. Biotechniques 31:120-126, 128, 130.

Tsuda H, Jafar-Nejad H, Patel AJ, Sun Y, Chen H-K, Rose MF, Venken KJT, Botas J, Orr HT, Bellen HJ, Zoghbi HY (2005) The AXH Domain of Ataxin-1 Mediates Neurodegeneration through Its Interaction with Gfi-1/Senseless Proteins. Cell 122:633-644.

Ward CL, Omura S, Kopito RR (1995) Degradation of CFTR by the ubiquitin-proteasome pathway. Cell 83:121-127.

Wing SS (2003) Deubiquitinating enzymes--the importance of driving in reverse along the ubiquitin-proteasome pathway. The International Journal of Biochemistry & Cell Biology 35:590-605.

Xia H, Mao Q, Eliason SL, Harper SQ, Martins IH, Orr HT, Paulson HL, Yang L, Kotin RM, Davidson BL (2004) RNAi suppresses polyglutamine-induced neurodegeneration in a model of spinocerebellar ataxia. 10:816-820.

Zhai Q, Wang J, Kim A, Liu Q, Watts R, Hoopfer E, Mitchison T, Luo L, He Z (2003) Involvement of the Ubiquitin-Proteasome System in the Early Stages of Wallerian Degeneration. Neuron 39:217-225.

Zhang M, Thurig S, Tsirigotis M, Wong PKY, Reuhl KR, Gray DA (2003) Effects of Mutant Ubiquitin on ts1 Retrovirus-Mediated Neuropathology. J Virol 77:7193-7201.

Zhuchenko O, Bailey J, Bonnen P, Ashizawa T, Stockton DW, Amos C, Dobyns WB, Subramony SH, Zoghbi HY, Lee et a (1997) Autosomal dominant cerebellar ataxia (SCA6) associated with small polyglutamine expansions in the alpha 1A-voltage-dependent calcium channel. Nature Genetics 15:62-69.

Zu T, Duvick LA, Kaytor MD, Berlinger MS, Zoghbi HY, Clark HB, Orr HT (2004) Recovery from polyglutamine-induced neurodegeneration in conditional SCA1 transgenic mice. J Neurosci 24:8853-8861.

Statement of contribution of collaborators

Immunohistochemisty and immunofluorescence described in the thesis was performed by Mei Zhang. Animal rotarod experiments and neuronal cell cultures were generated by Melissa Beyers. Ubiquitin transgenic mice were characterized my Maria Tsirigotis. The radio-active probe for Northern blot analysis was prepared by Maria Tsirigotis. She also assisted in protein extraction and Western blot analysis of mouse cerebella. All photographs were taken by Dr. Douglas Gray.

My contributions to Tsirigotis et al., 2005 (in press) include the excision of mouse cerebella, subsequent extraction of RNA and performing transcriptional analysis by quantitative RT-PCR. I also assisted with the preparation of tissue extracts used in western blot analysis. I performed some western blots on p300/CBP, PCAF and acetylated H4.